Numerical experiment 9

Material parameters:

Os: Young's modulus $E = 1,71 \times 10^{10}$[Pa] and Poisson's ratio $\nu = 0,25$.
(1) Ti6Al4V: Young's modulus $E = 1,15 \times 10^{11}$[Pa] and Poisson's ratio $\nu = 0,3$.
(2) Chirulen: Young's modulus $E = 3,4 \times 10^{8}$[Pa] and Poisson's ratio $\nu = 0,4$.
(3) CoCrMo: Young's modulus $E = 2,08 \times 10^{11}$[Pa] and Poisson's ratio $\nu = 0,3$.

Boundary conditions:

Model I

Prescribed zero displacement on 1-2, 3-4.
Unilateral contact boundary on 7-8.
Pressure $1,45 \times 10^{6}$[Pa] on 5-6 ..... Model I-A
Pressure $1,52 \times 10^{6}$[Pa] on 5-6 ..... Model I-B
Pressure $1,61 \times 10^{6}$[Pa] on 5-6 ..... Model I-C

Model II

Prescribed zero displacement on 1-2.
Unilateral contact boundary on 7-8.
Pressure $1,2 \times 10^{6}$[Pa] on 5-6 ..... Model II-A
Pressure $1,0 \times 10^{6}$[Pa] on 5-6 ..... Model II-B
Pressure $0,8 \times 10^{6}$[Pa] on 5-6 ..... Model II-C

Discretization statistics:

Model I

10 subdomains, 2867 nodes, 4740 elements,
33 unilateral contact conditions, 299 interface elements.

Model II

8 subdomains, 2474 nodes, 4104 elements,
33 unilateral contact conditions, 290 interface elements.

Description:

Model I - the outer cut in the sagital plane

Model II - the inner cut in the sagital plane

Model I-A and II-A - correspond to the case of mechanical axis with deviation 5 degrees in the frontal plane
Model I-B and II-B - correspond to the case of mechanical axis with deviation 7 degrees in the frontal plane
Model I-C and II-C - correspond to the case of mechanical axis with deviation 9 degrees in the frontal plane

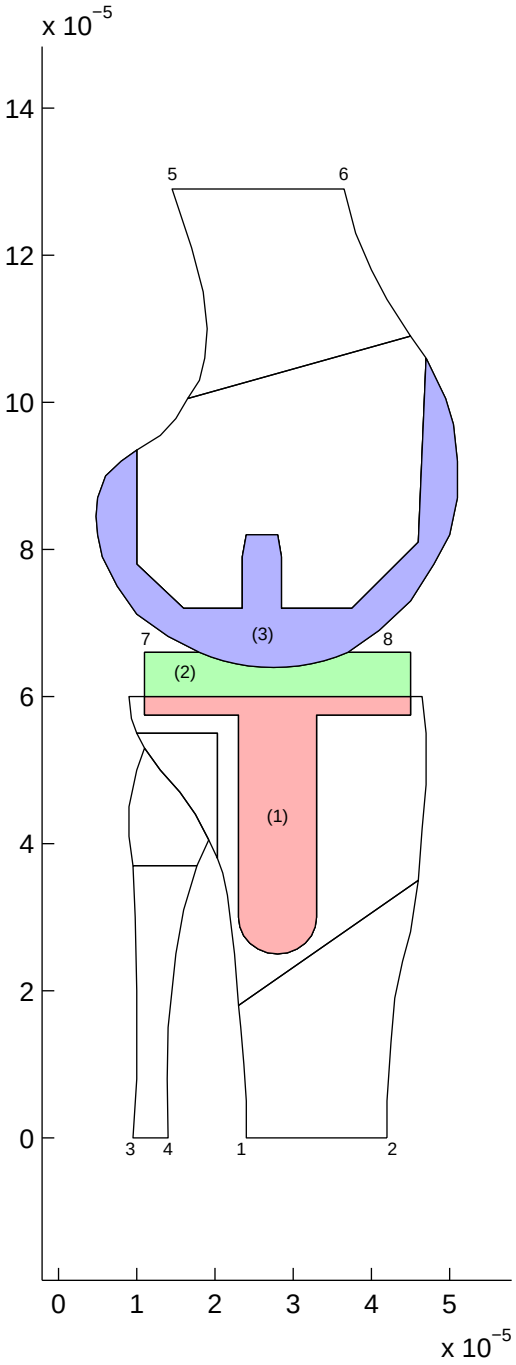

Figure 99: The geometry of the model I

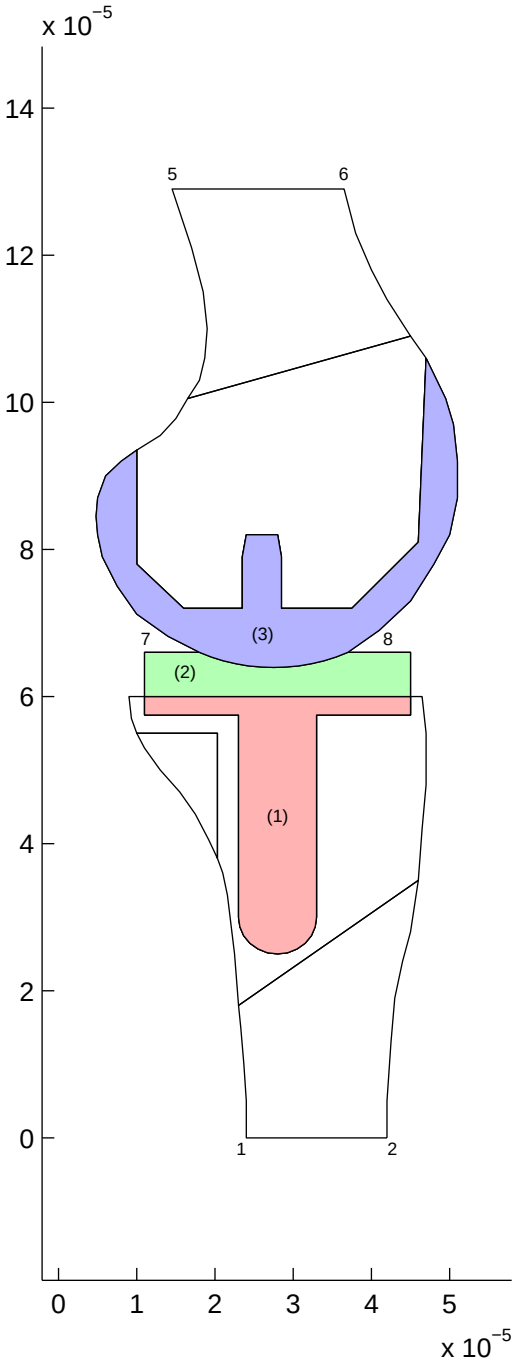

Figure 100: The geometry of the model II

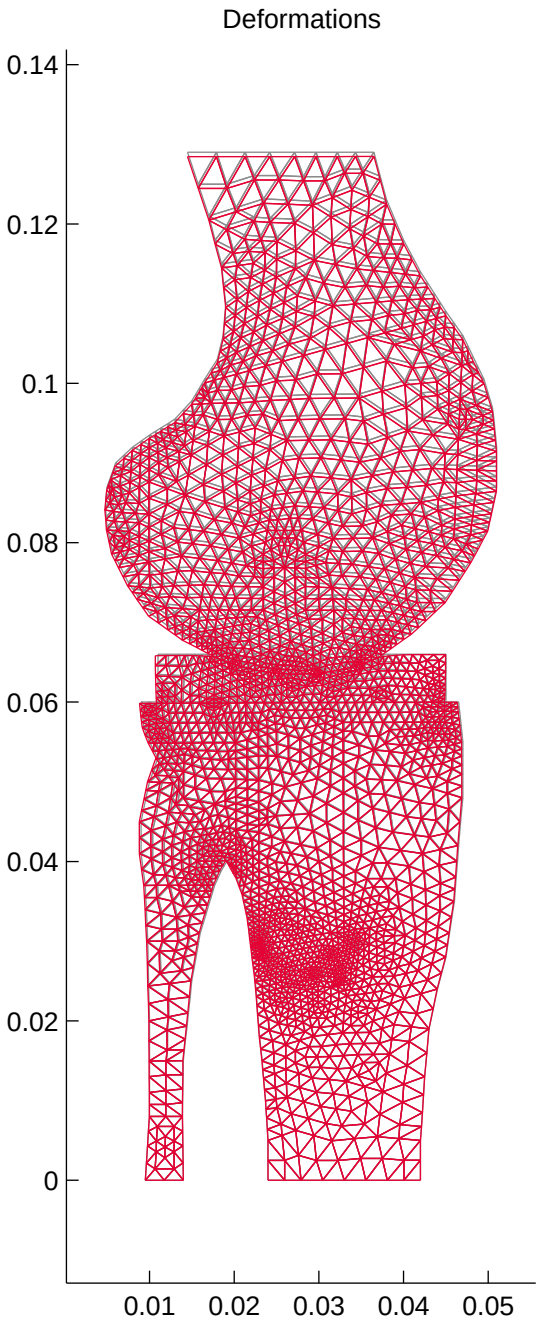

Figure 101: Model I-A - Deformations (enlarge factor=20)

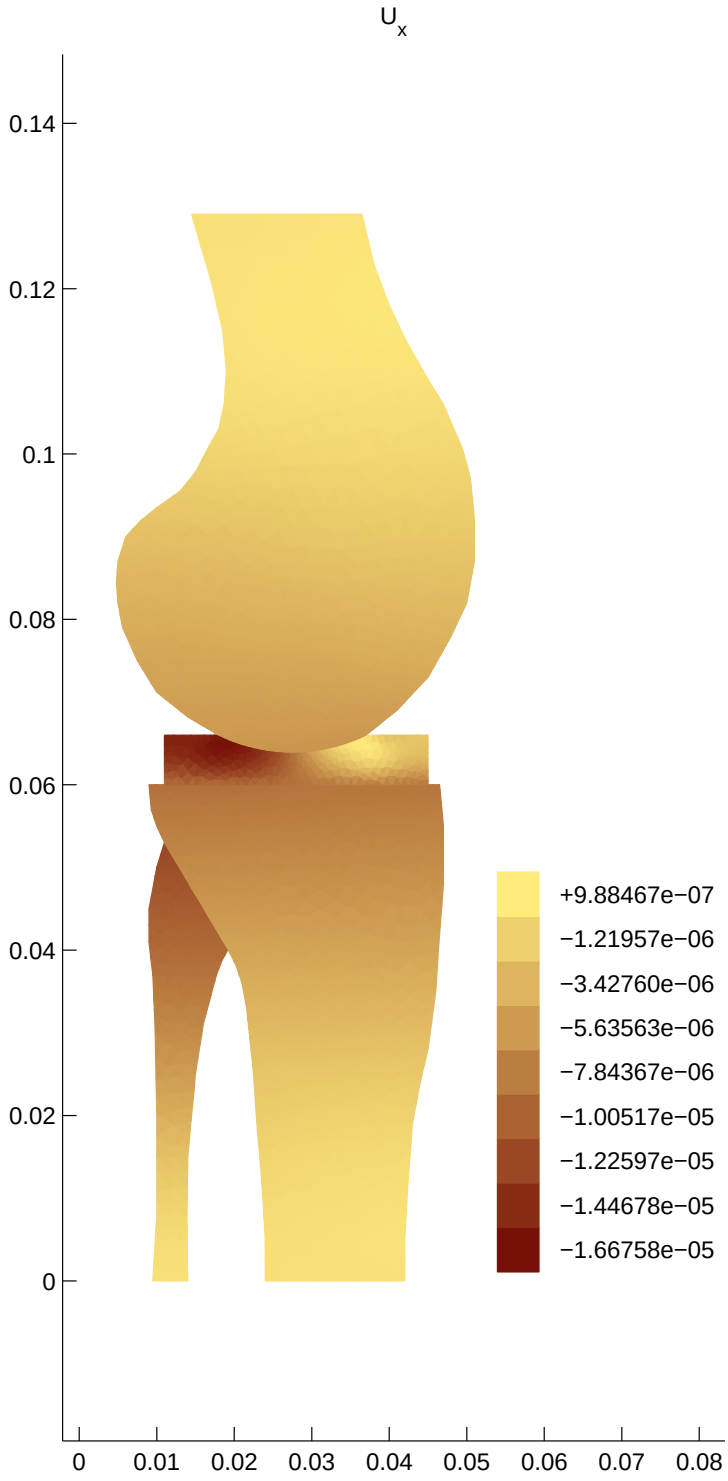

Figure 102: Model I-A - Horizontal component of displacement

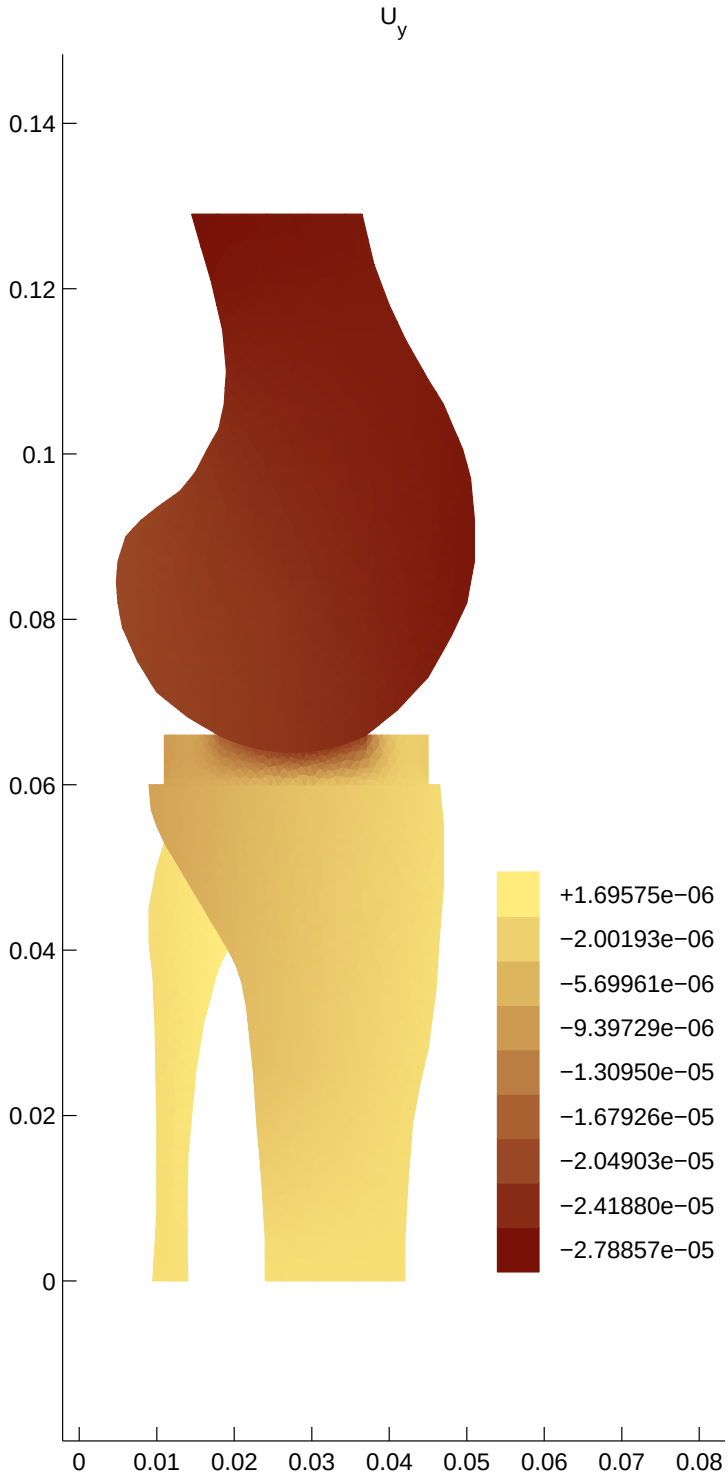

Figure 103: Model I-A - Vertical component of displacement

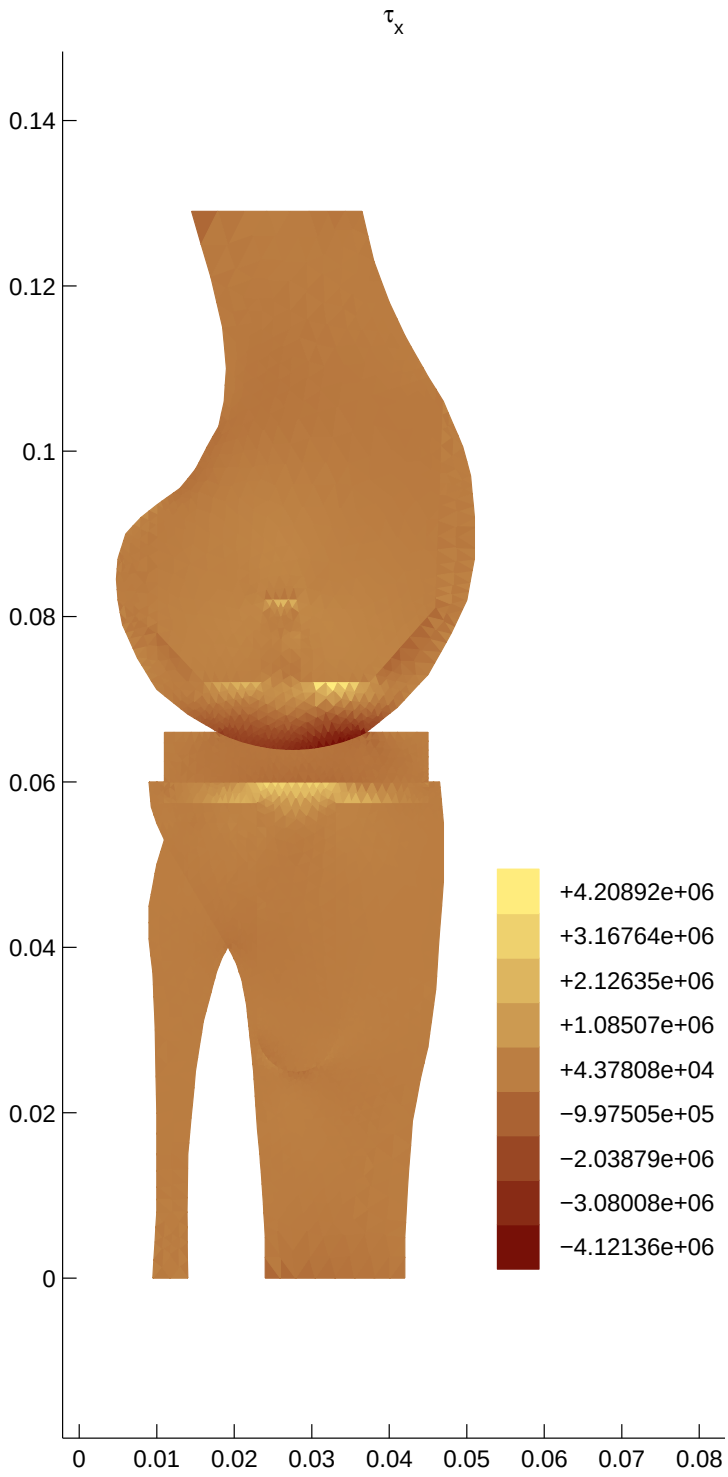

Figure 104: Model I-A - Stresses τ_x

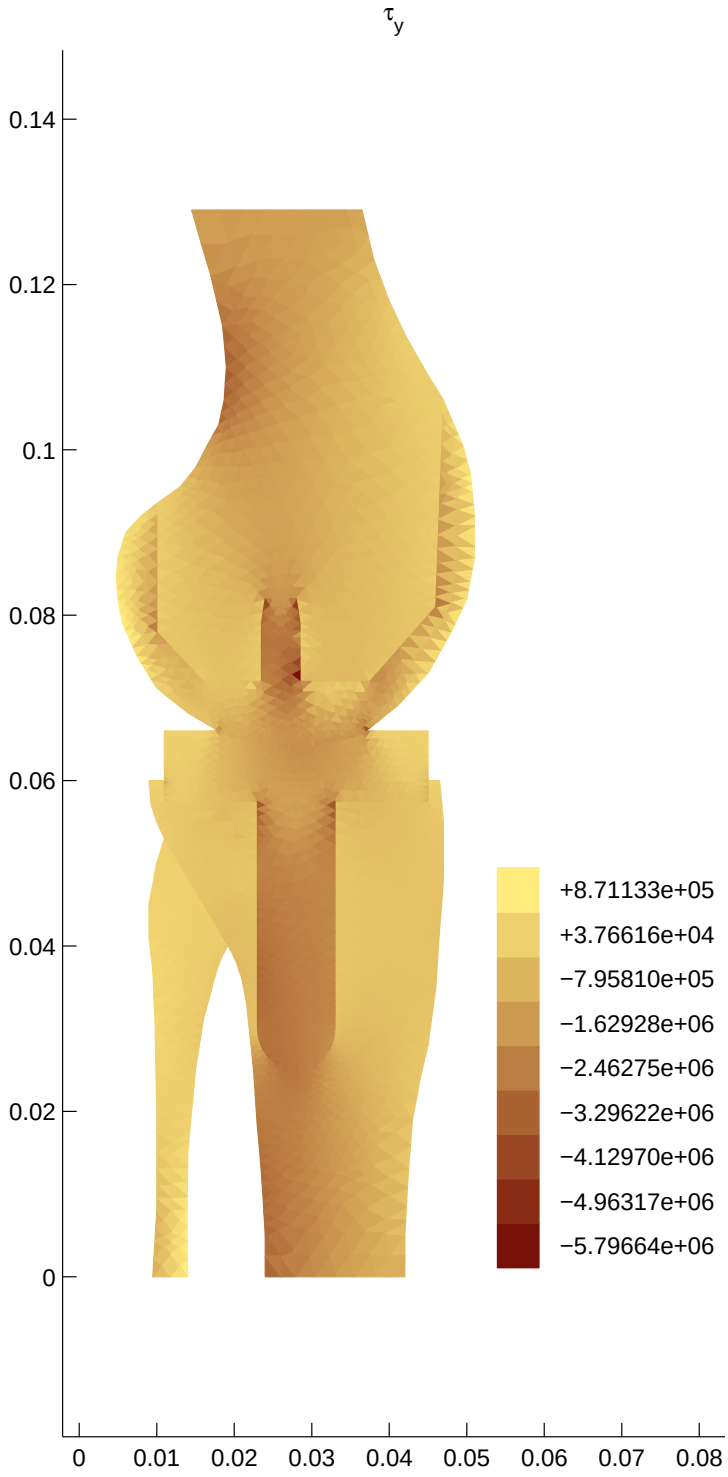

Figure 105: Model I-A - Stresses τ_y

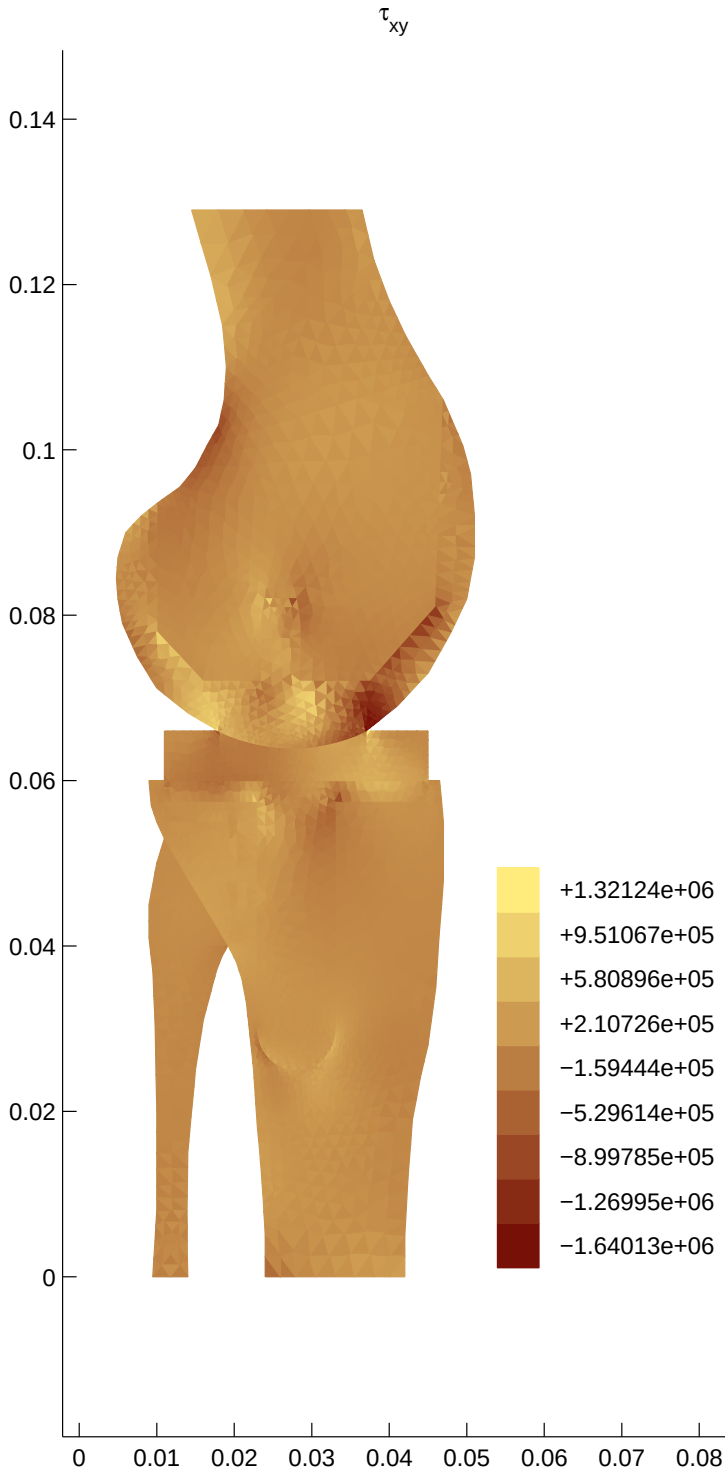

Figure 106: Model I-A - Stresses τ_{xy}

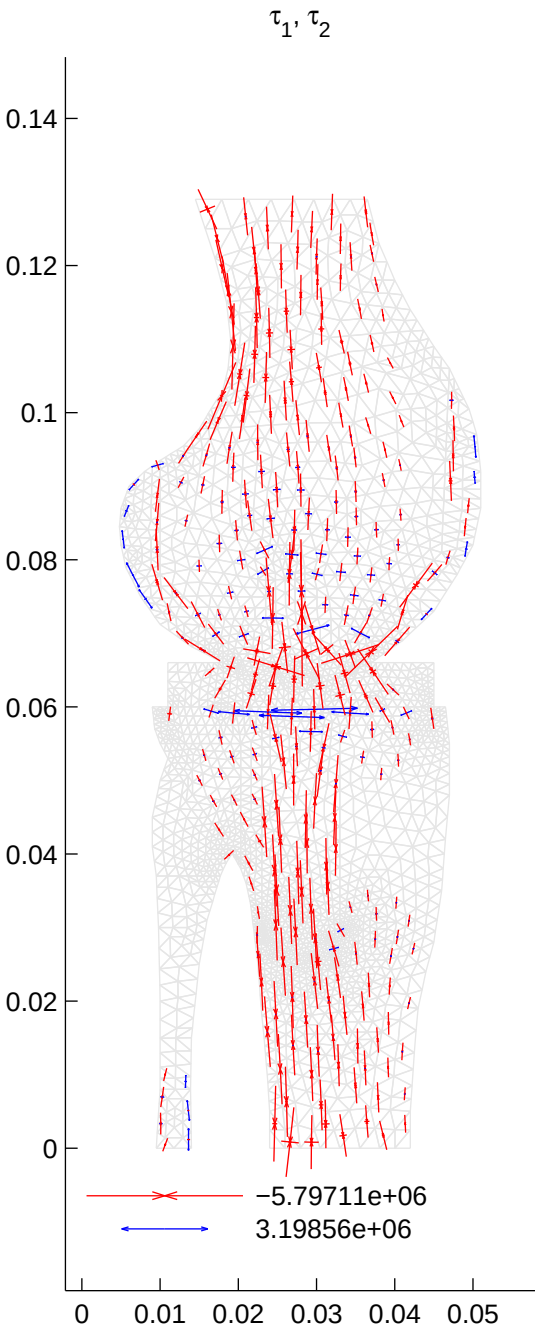

Figure 107: Model I-A - Principal stresses

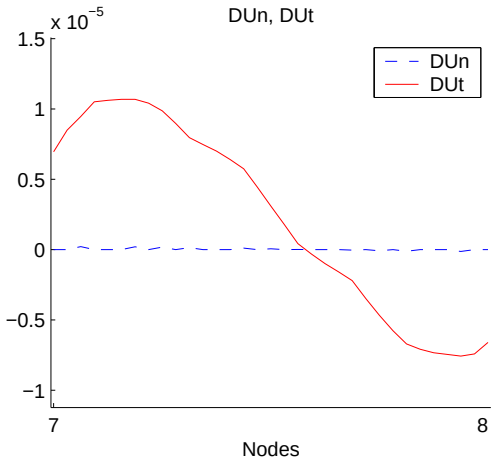

Figure 108: Model I-A - The normal and tangential components of displacement on the contact boundary

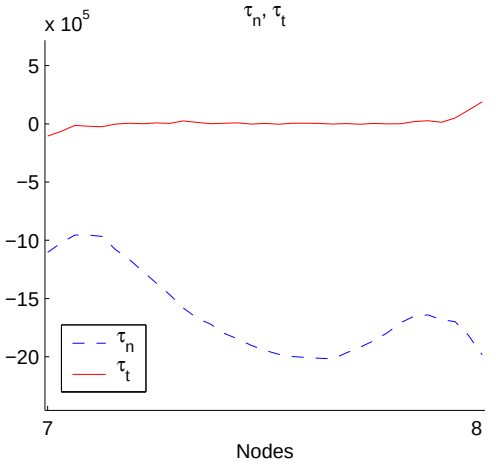

Figure 109: Model I-A - The normal and tangential components of stress vector on the contact boundary

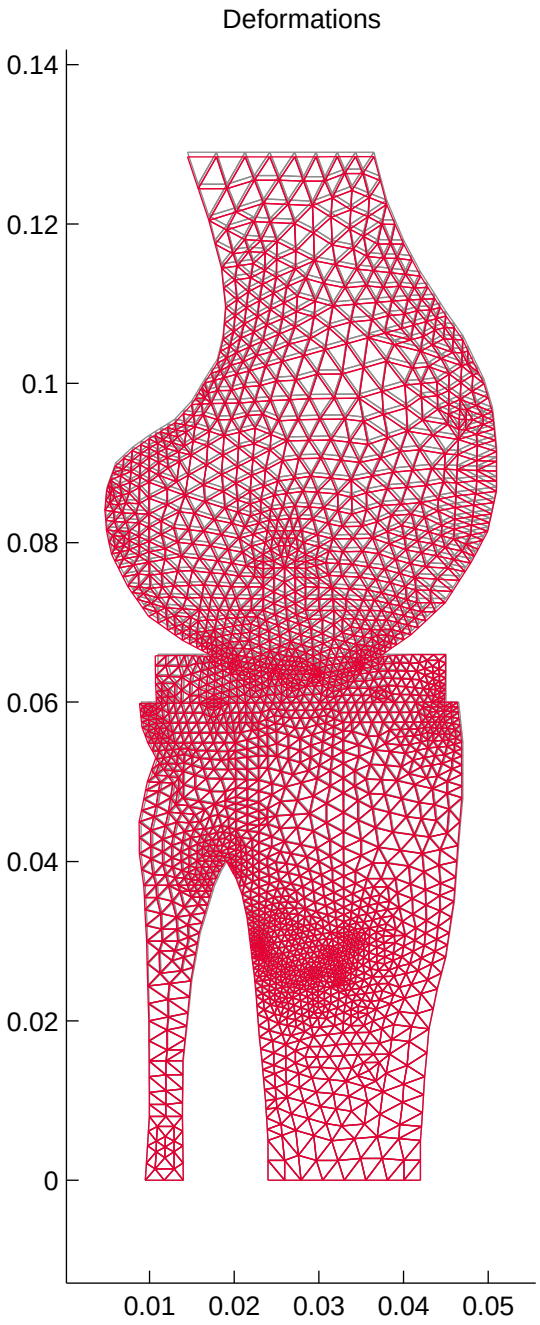

Figure 110: Model I-B - Deformations (enlarge factor=20)

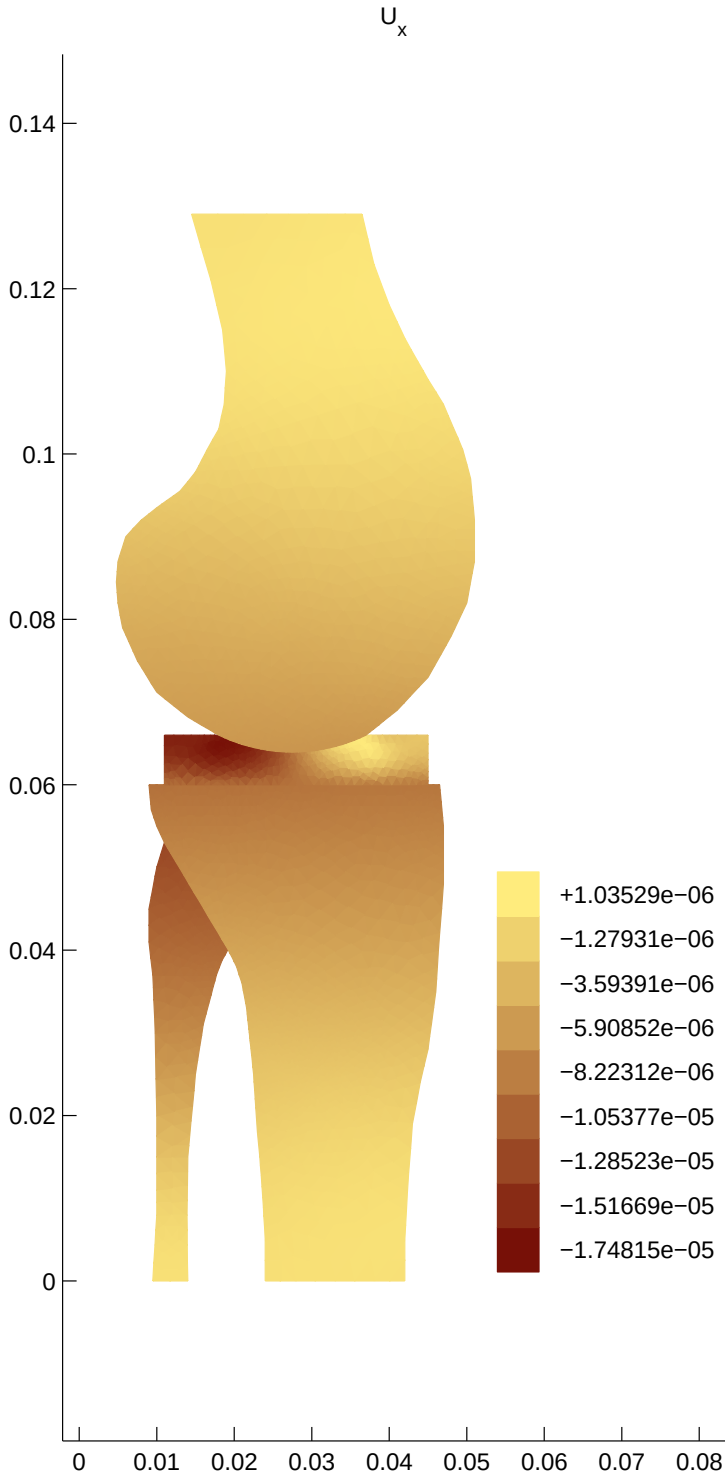

Figure 111: Model I-B - Horizontal component of displacement

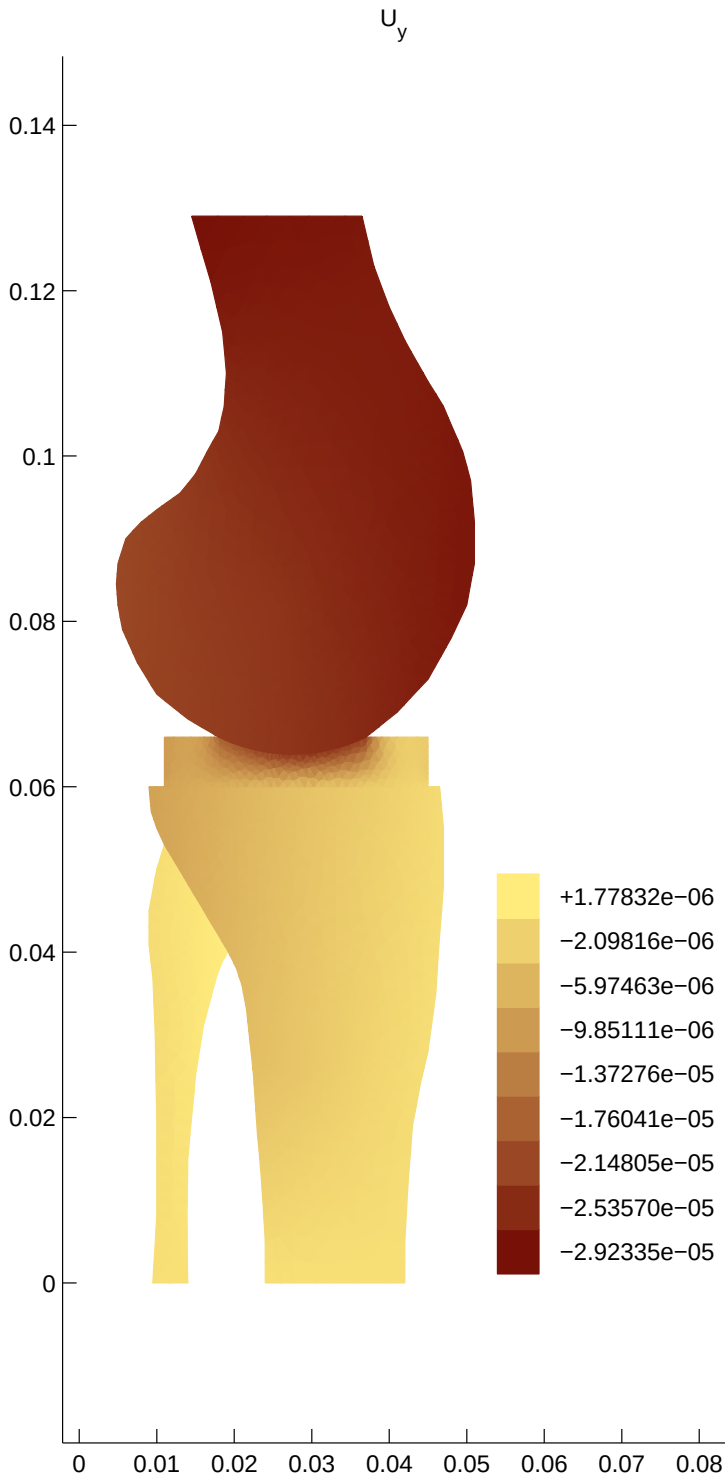

Figure 112: Model I-B - Vertical component of displacement

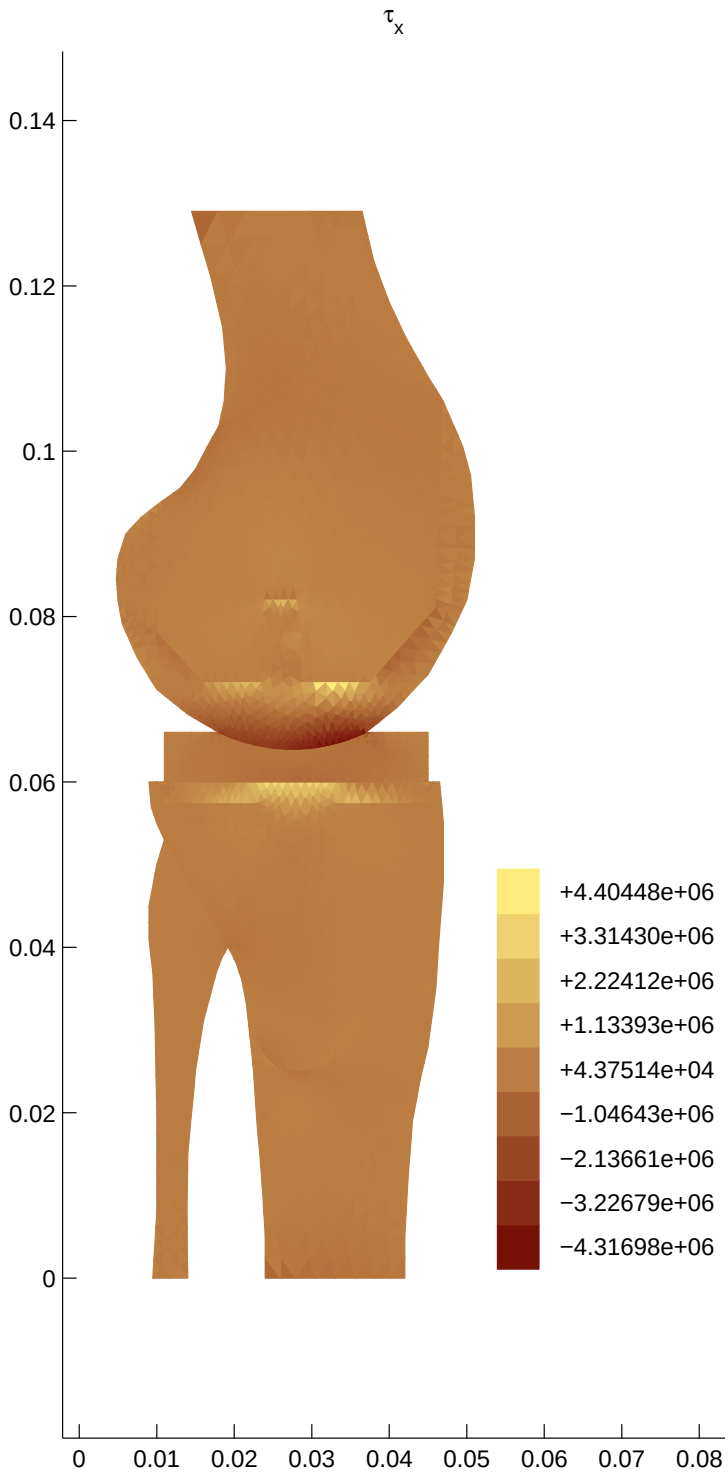

Figure 113: Model I-B - Stresses τ_x

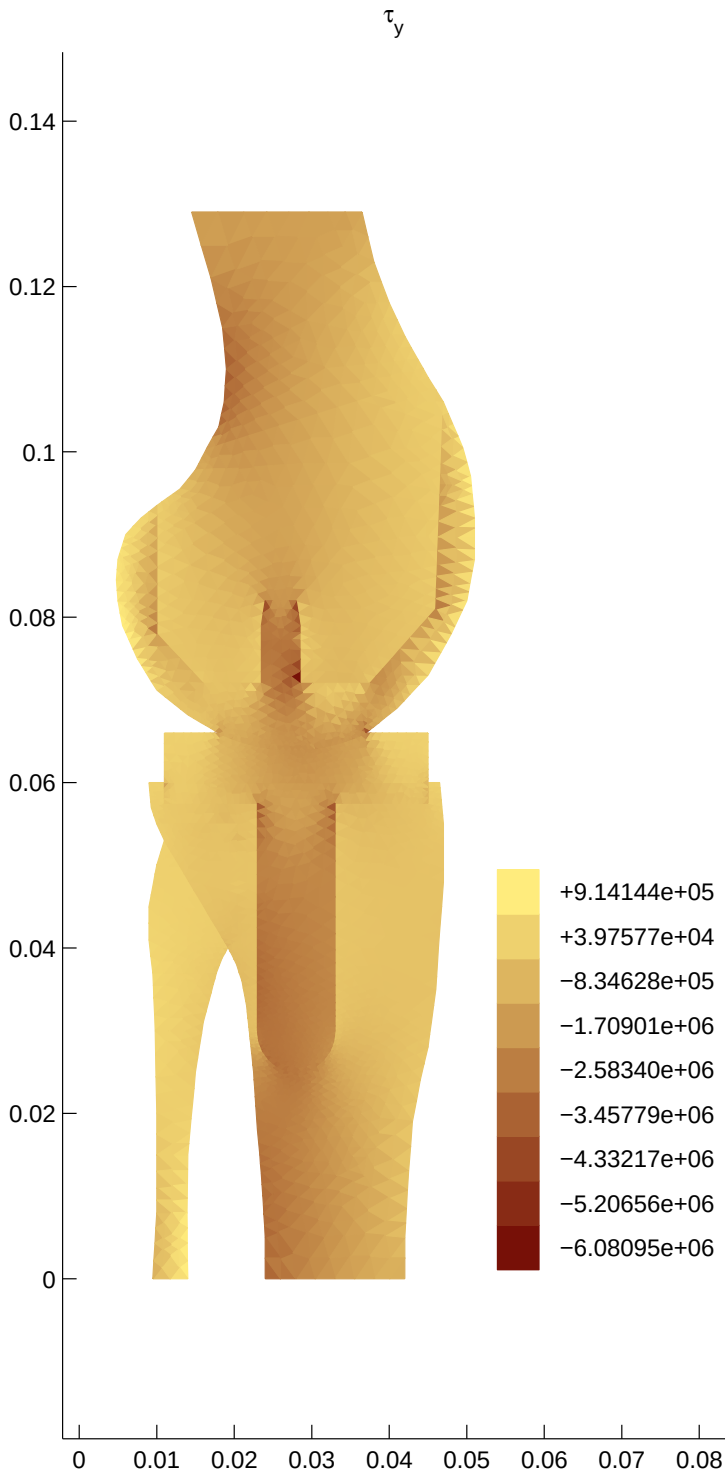

Figure 114: Model I-B - Stresses τ_y

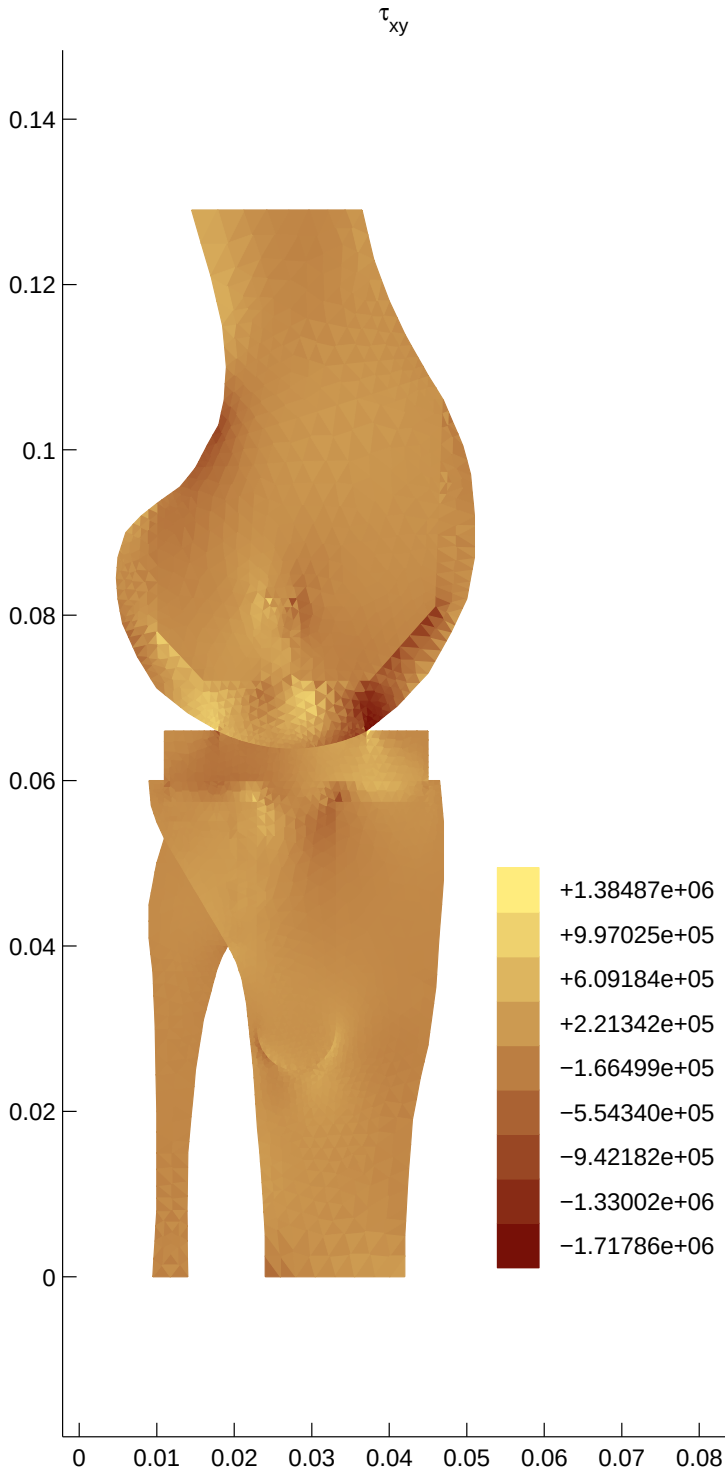

Figure 115: Model I-B - Stresses τ_{xy}

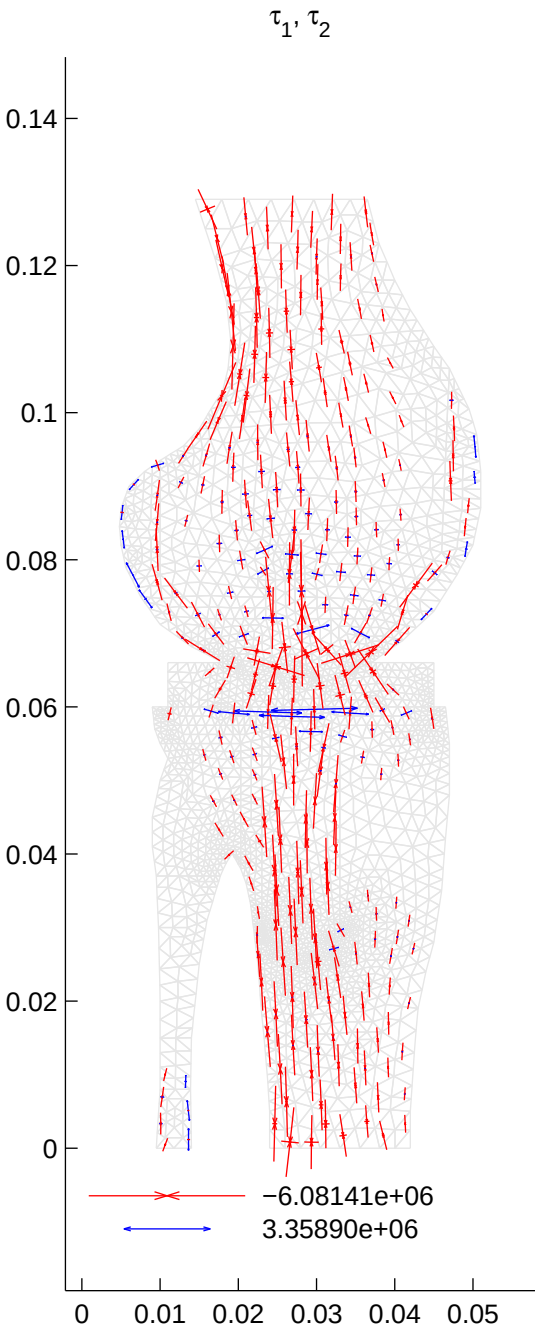

Figure 116: Model I-B - Principal stresses

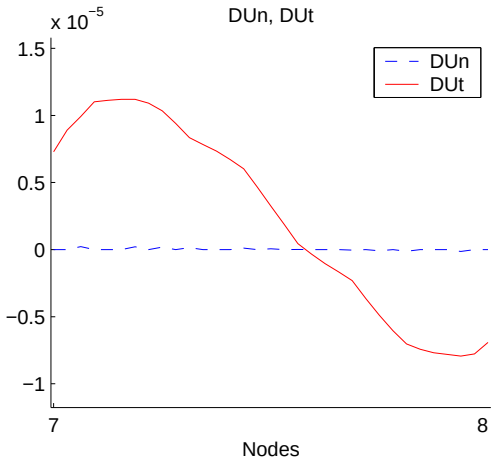

Figure 117: Model I-B - The normal and tangential components of displacement on the contact boundary

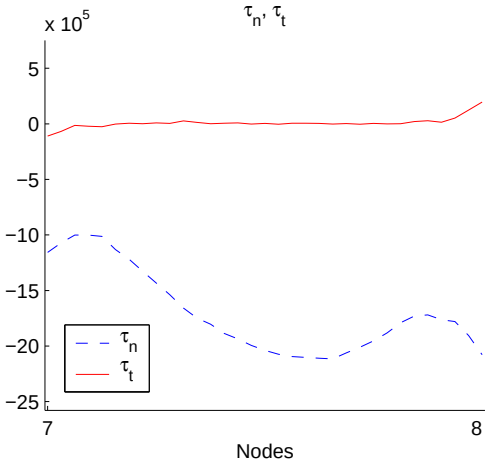

Figure 118: Model I-B - The normal and tangential components of stress vector on the contact boundary

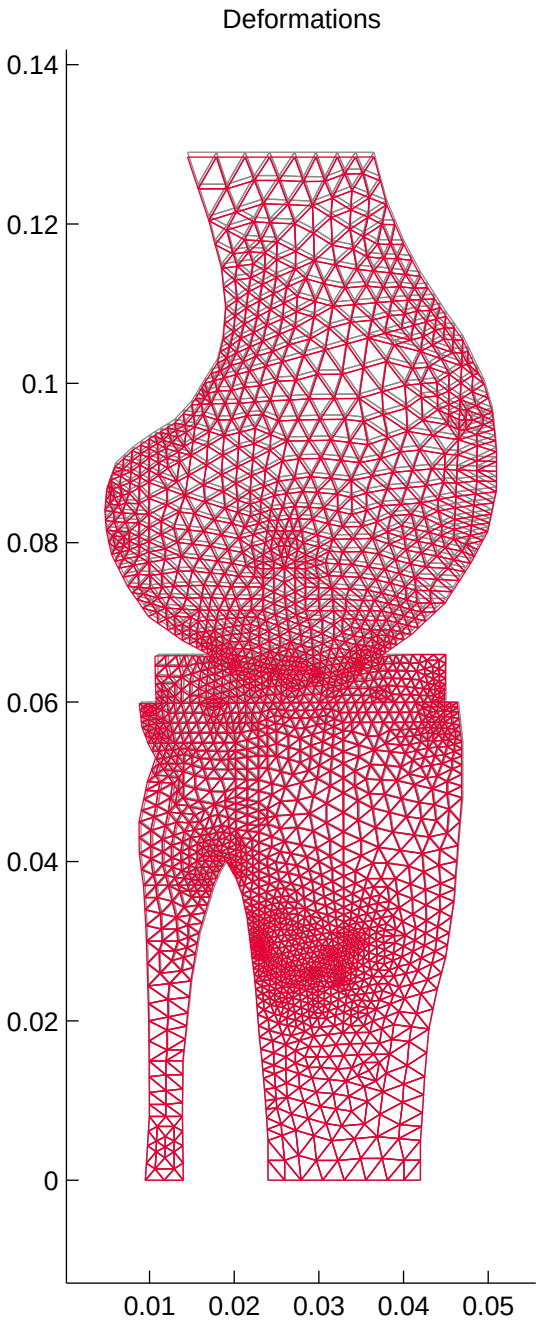

Figure 119: Model I-C - Deformations (enlarge factor=20)

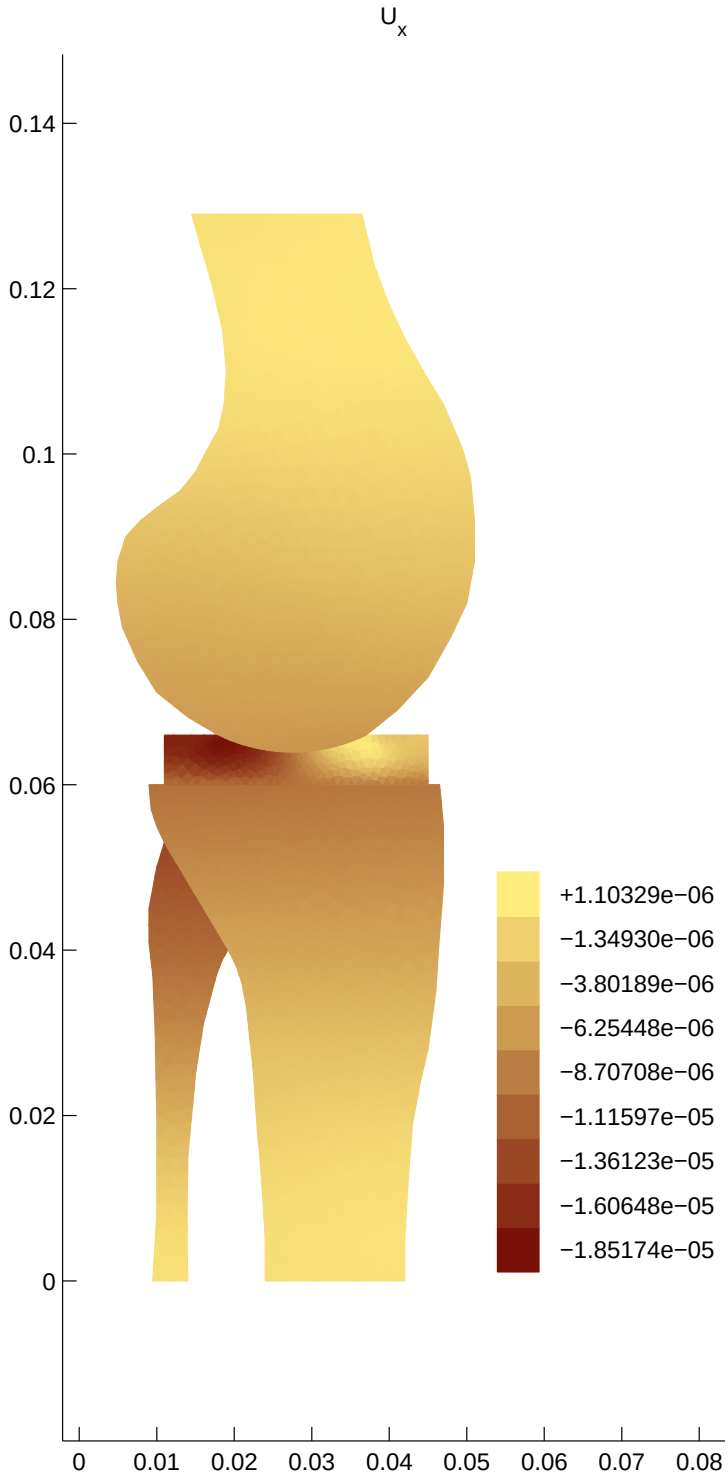

Figure 120: Model I-C - Horizontal component of displacement

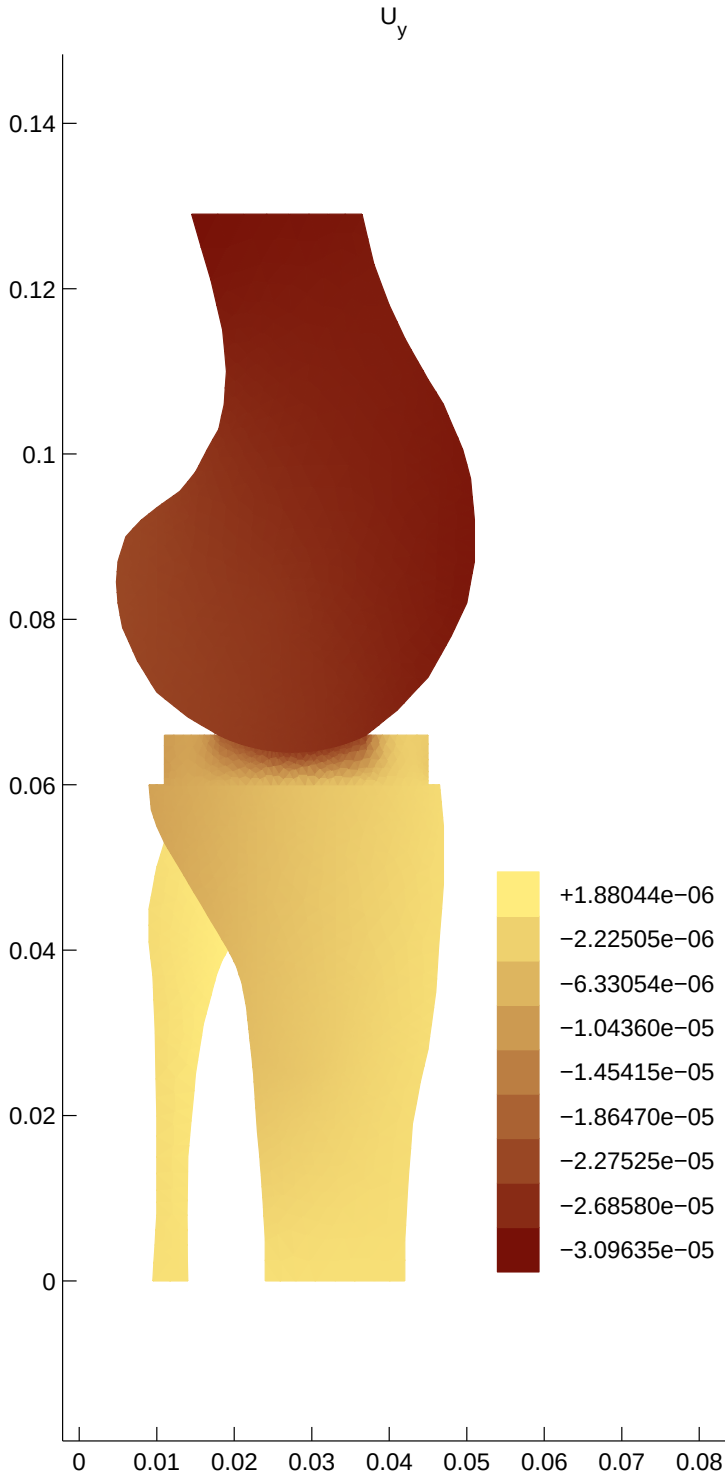

Figure 121: Model I-C - Vertical component of displacement

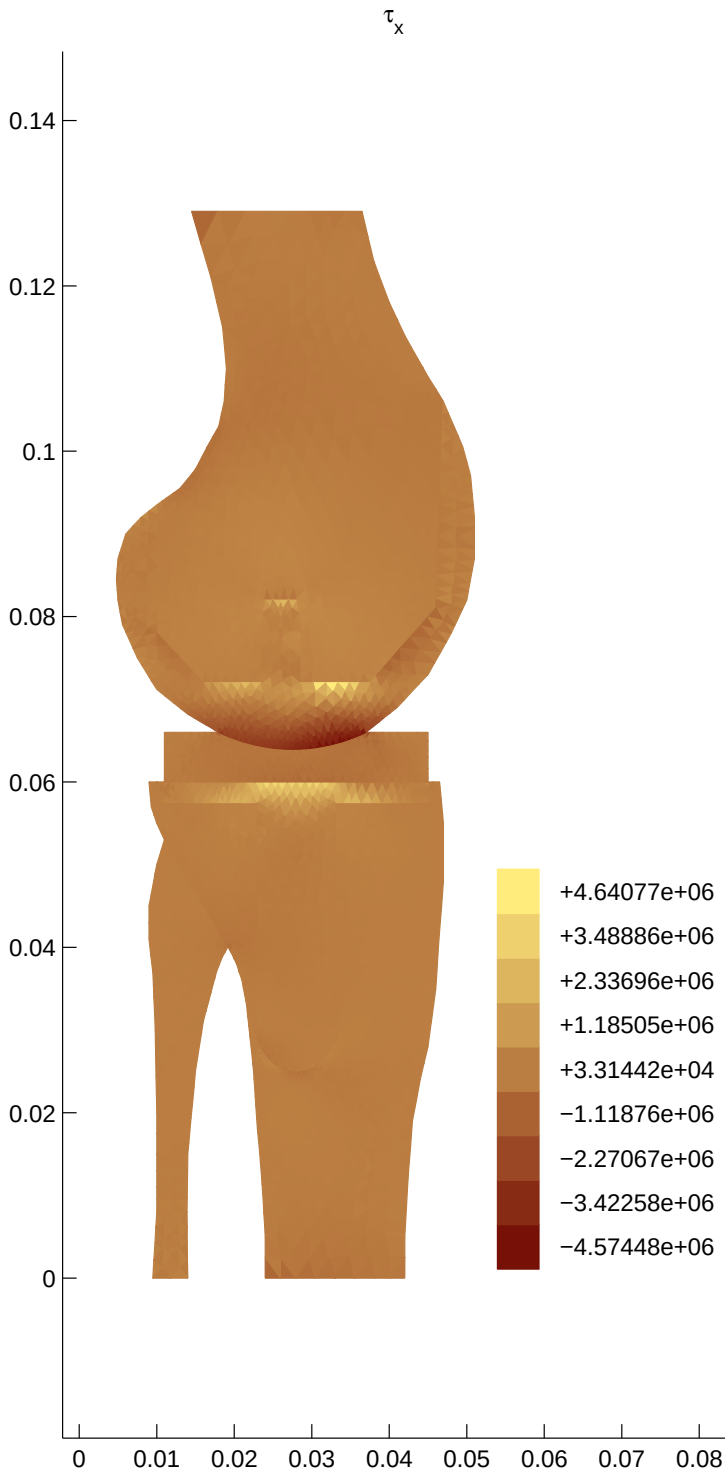

Figure 122: Model I-C - Stresses τ_x

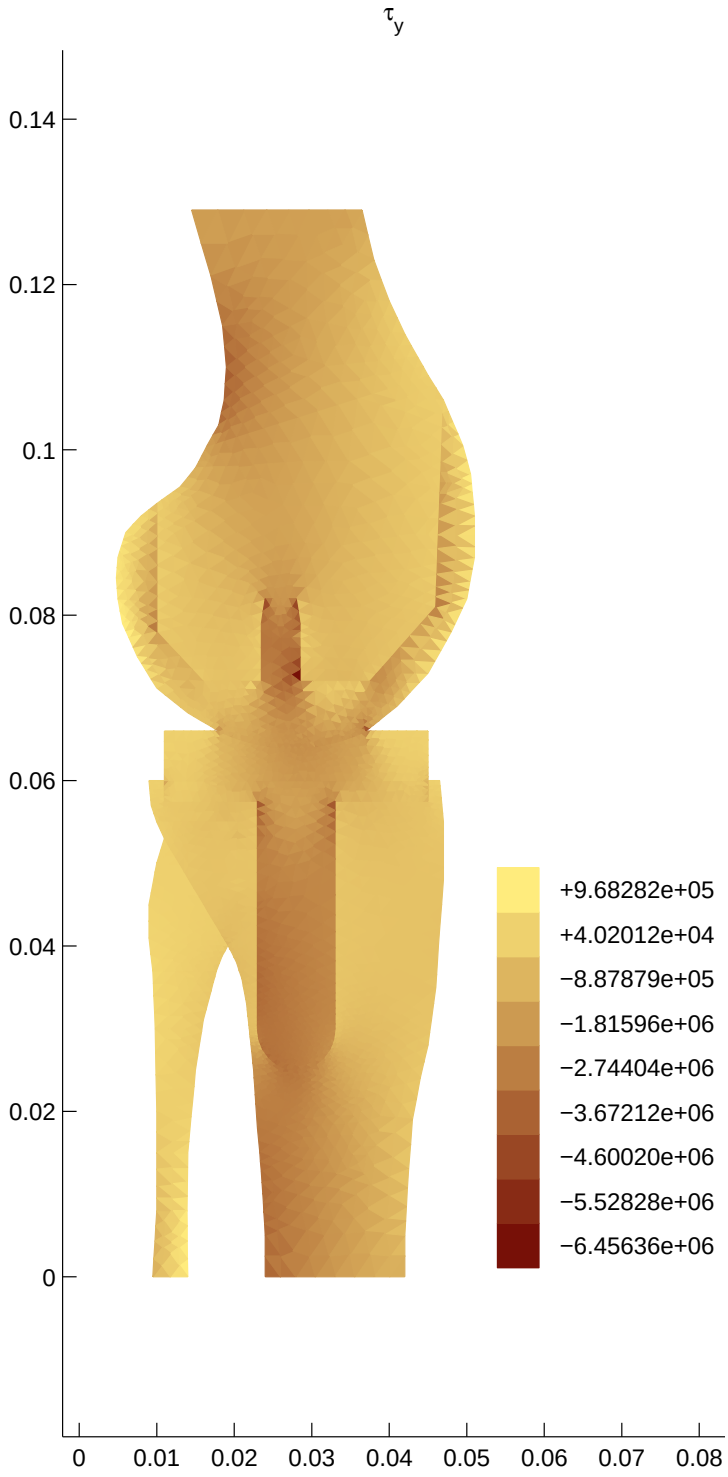

Figure 123: Model I-C - Stresses τ_y

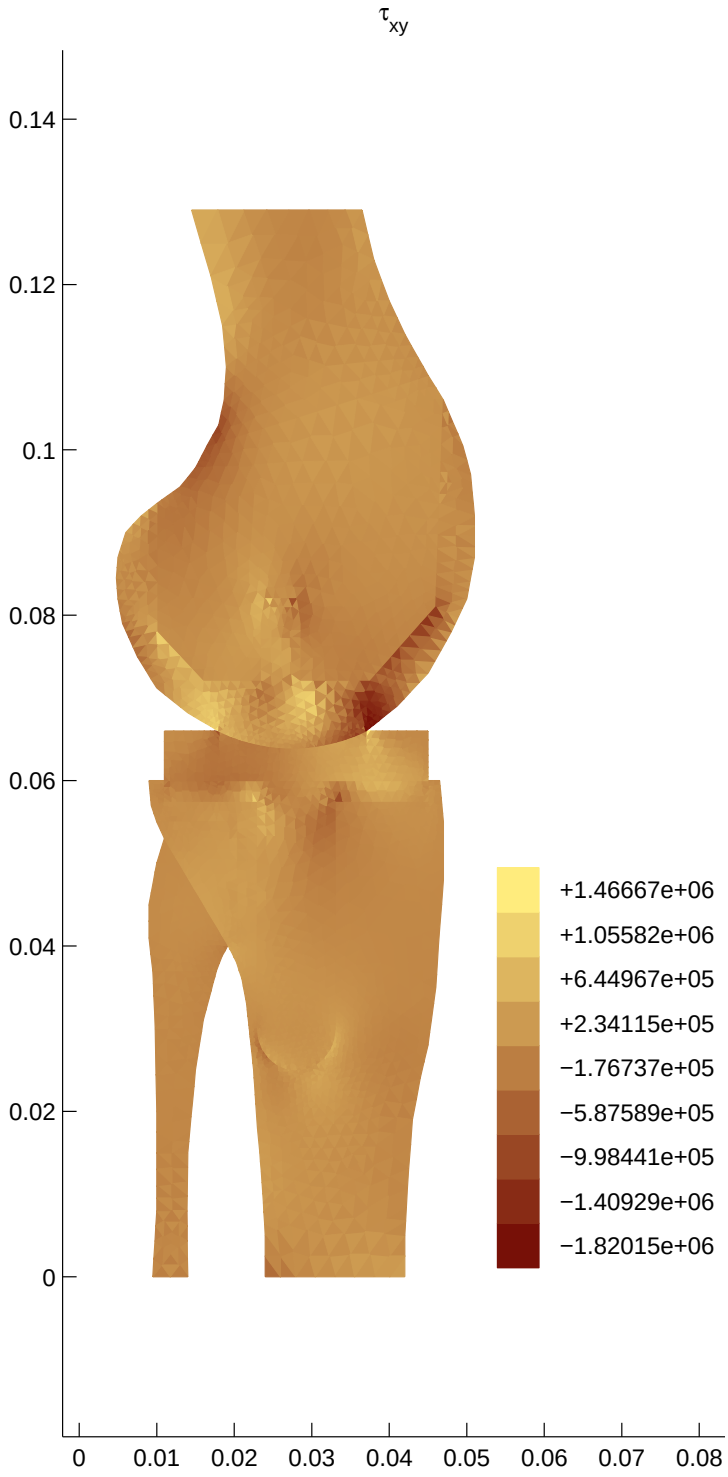

Figure 124: Model I-C - Stresses τ_{xy}

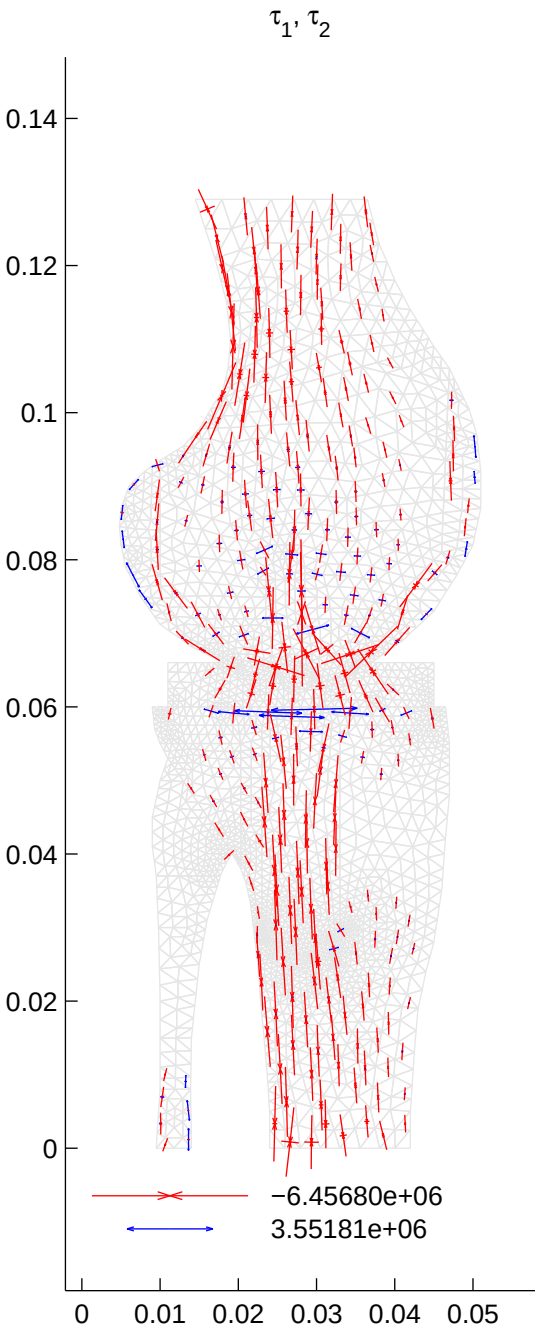

Figure 125: Model I-C - Principal stresses

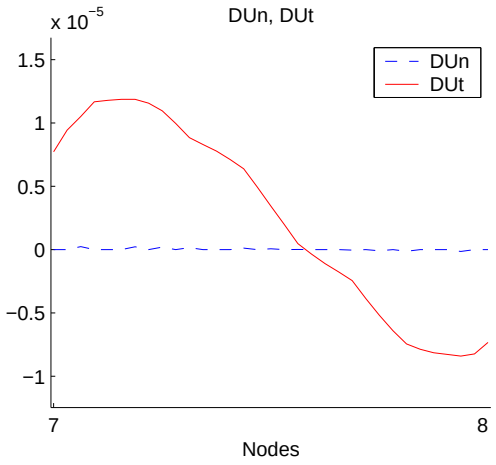

Figure 126: Model I-C - The normal and tangential components of displacement on the contact boundary

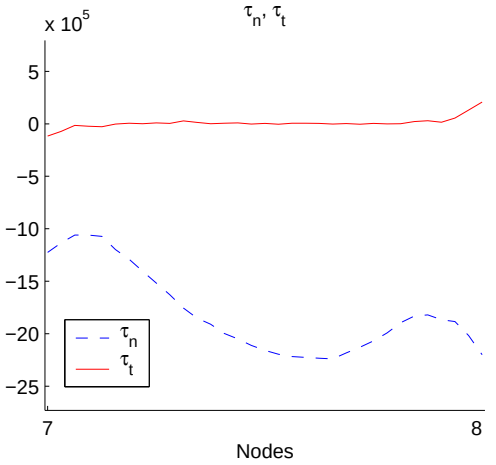

Figure 127: Model I-C - The normal and tangential components of stress vector on the contact boundary

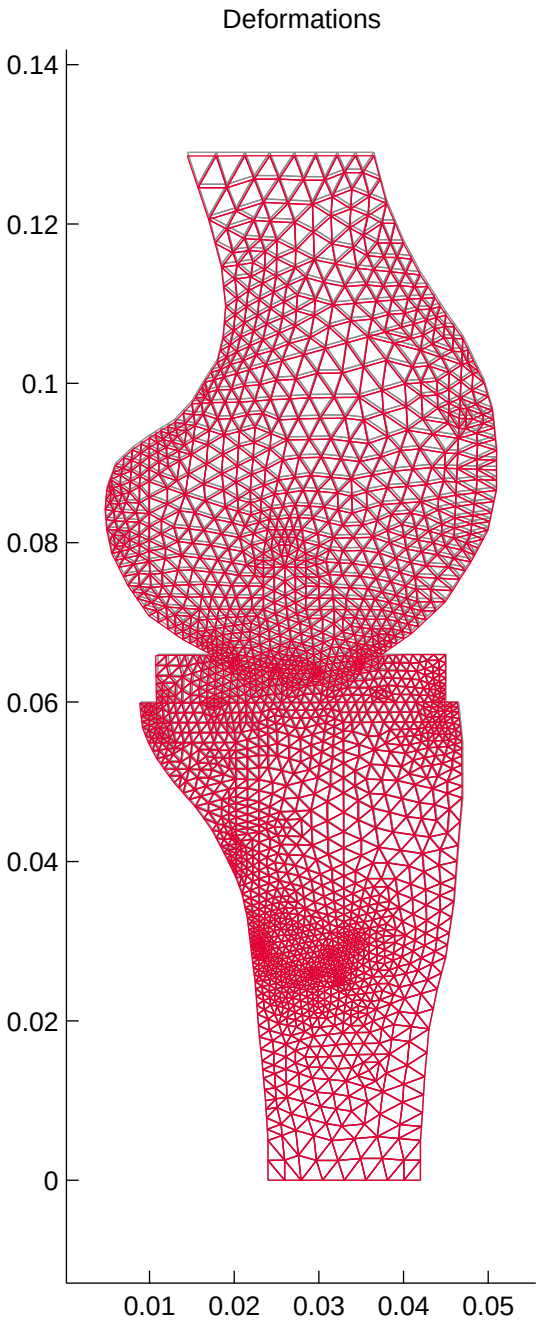

Figure 128: Model II-A - Deformations (enlarge factor=20)

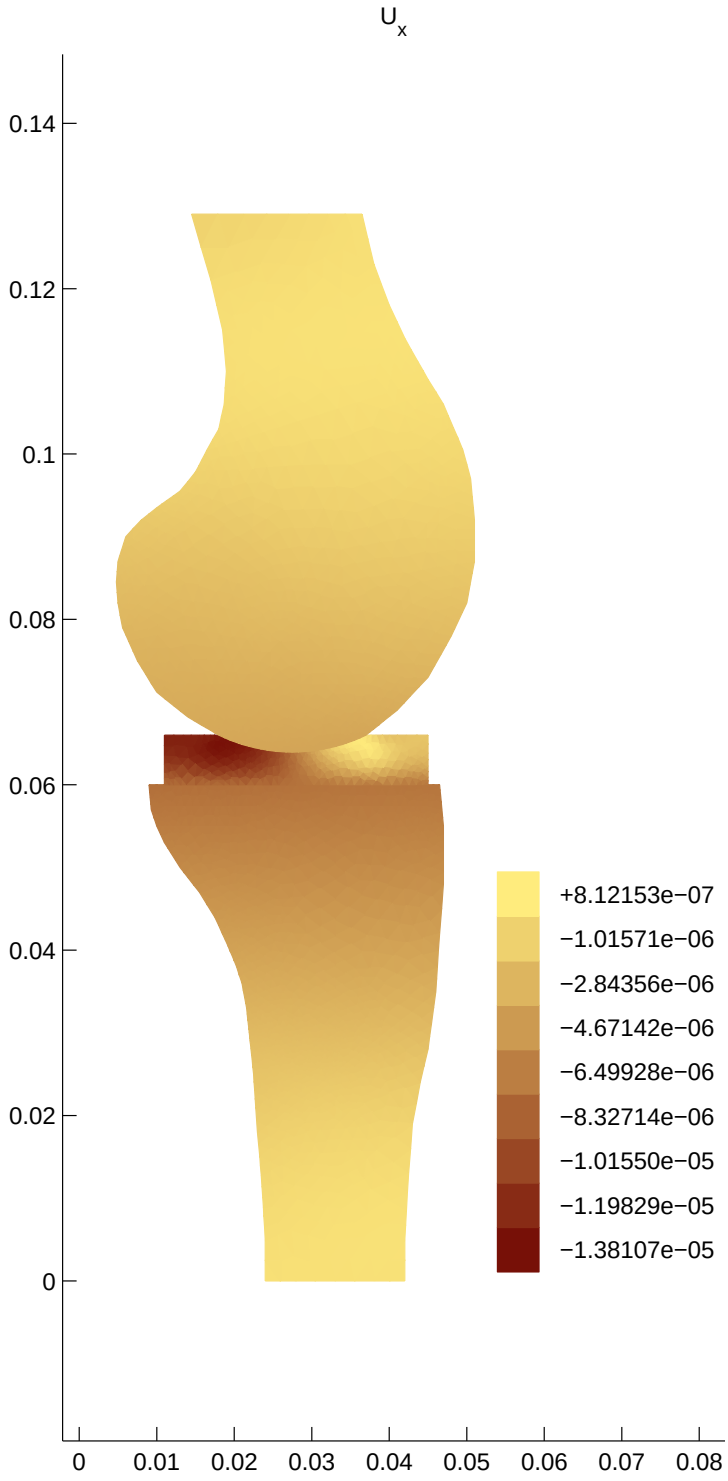

Figure 129: Model II-A - Horizontal component of displacement

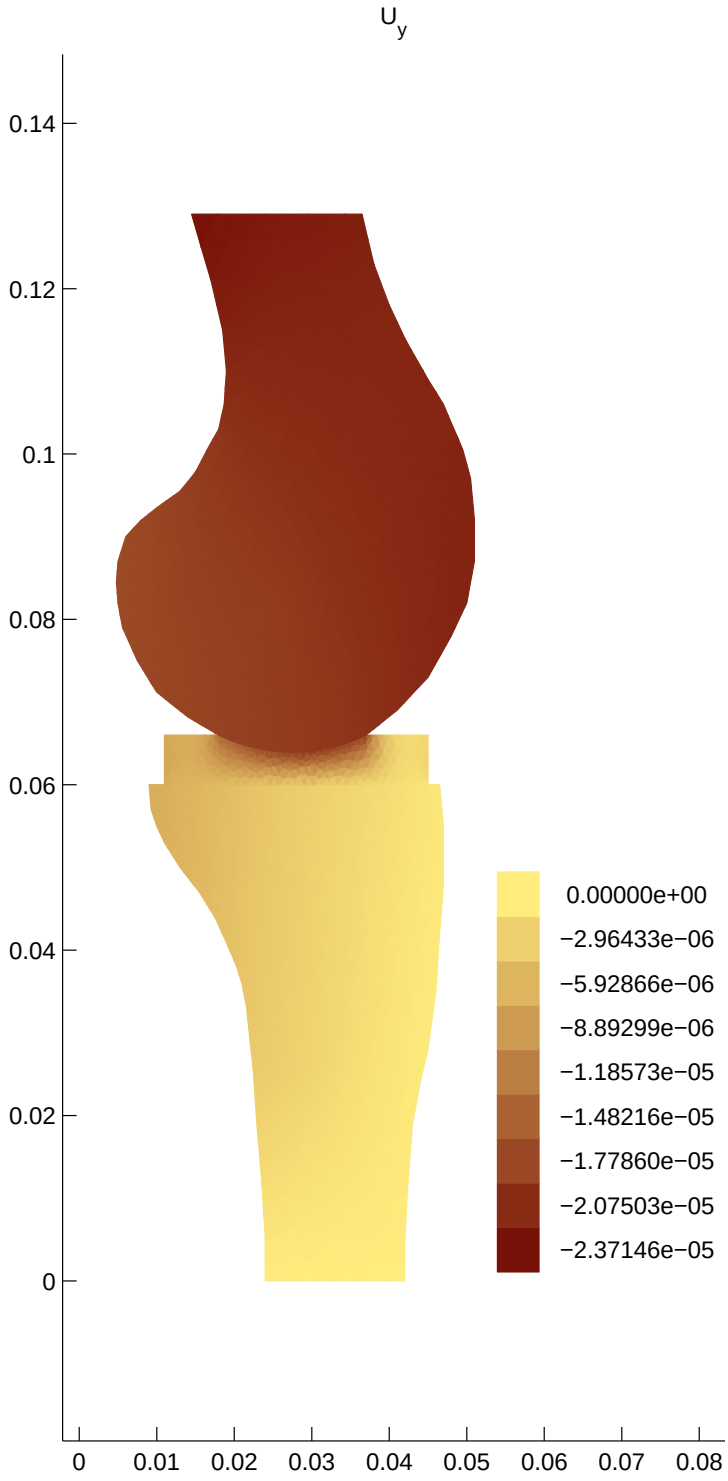

Figure 130: Model II-A - Vertical component of displacement

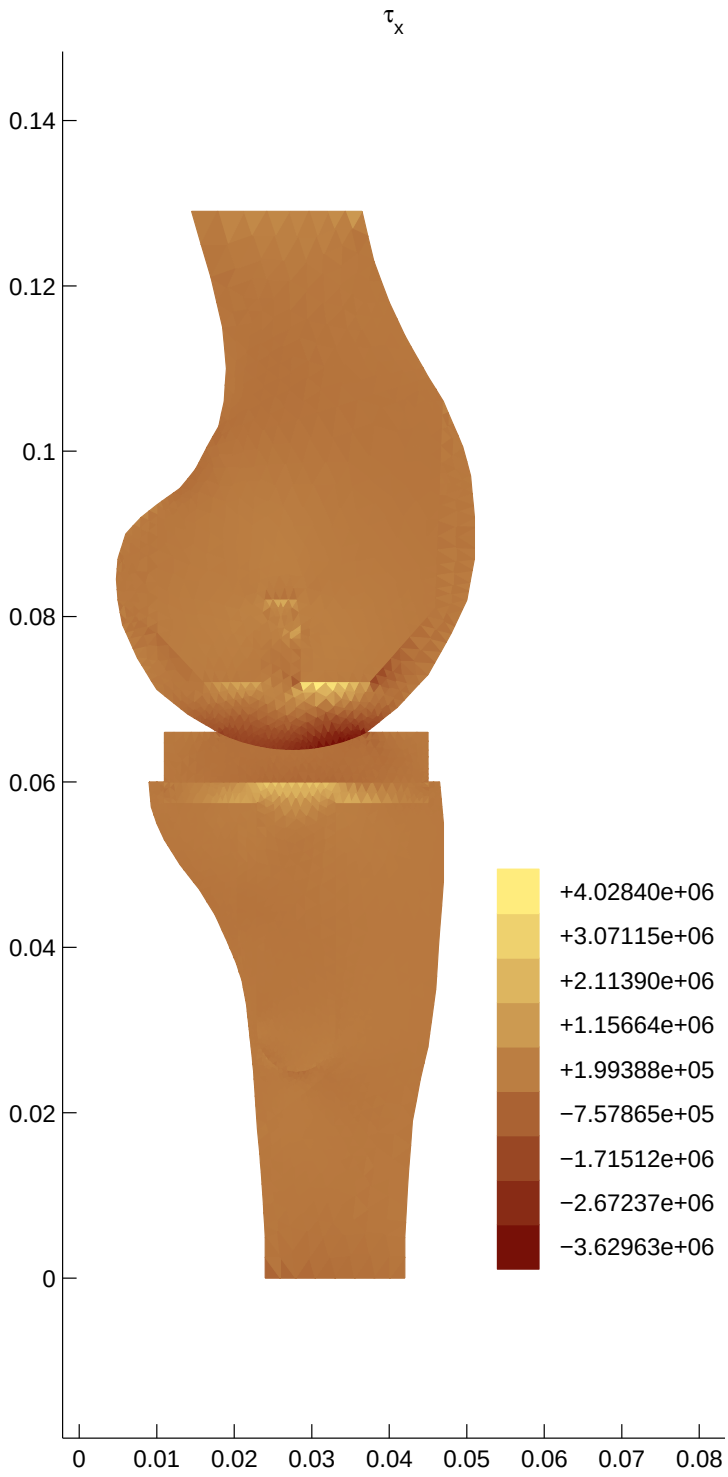

Figure 131: Model II-A - Stresses τ_x

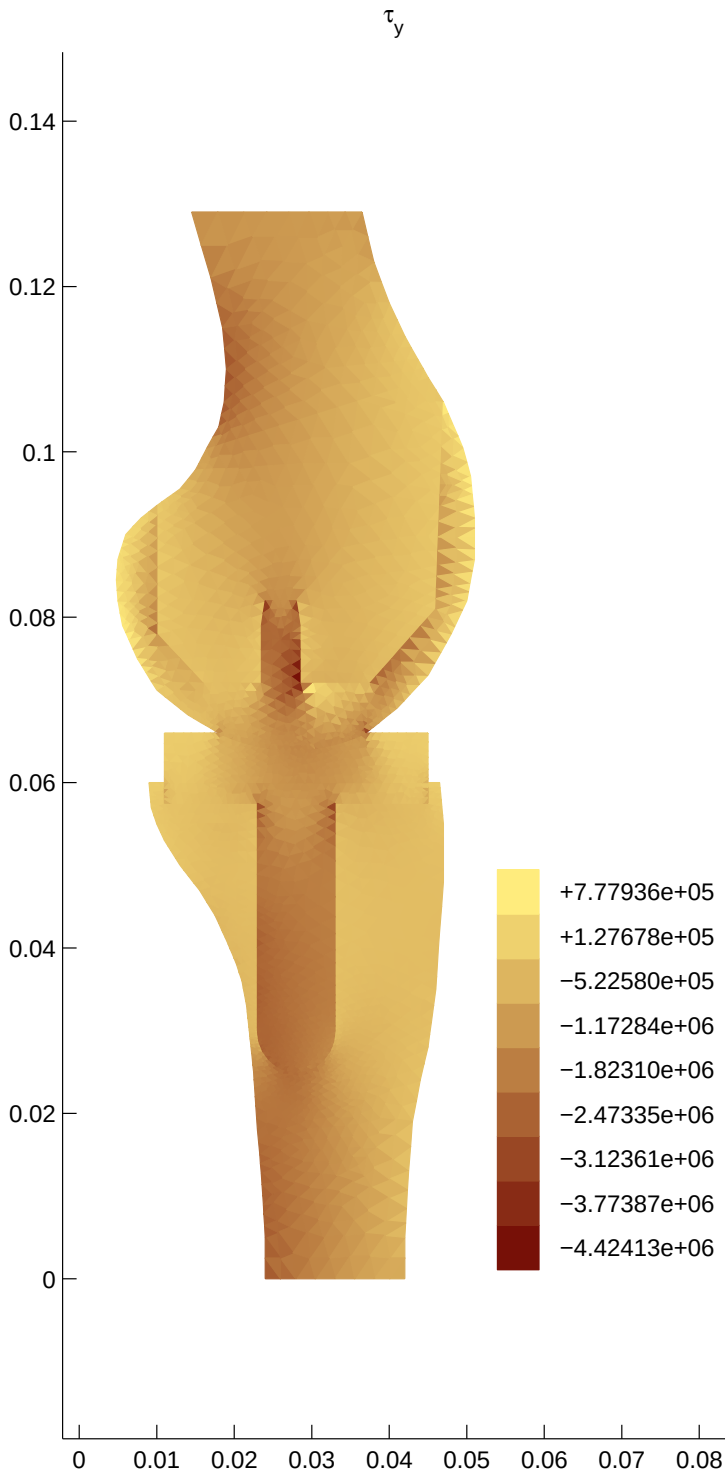

Figure 132: Model II-A - Stresses τ_y

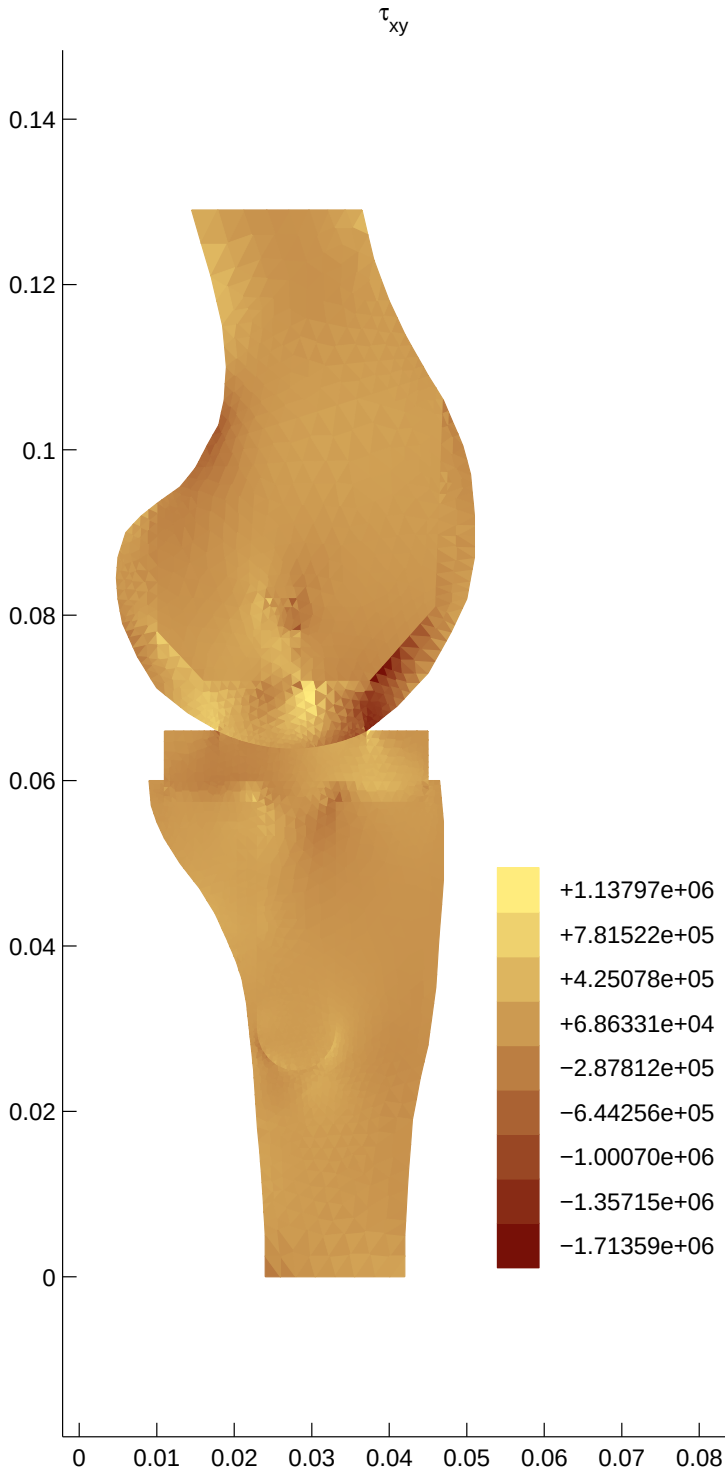

Figure 133: Model II-A - Stresses τ_{xy}

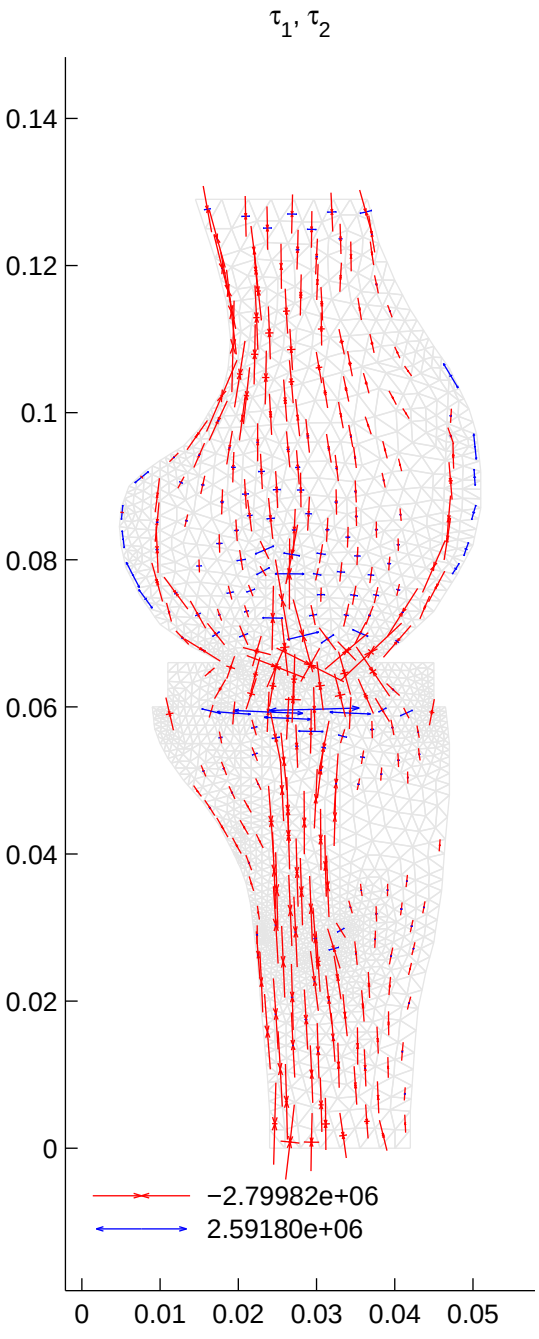

Figure 134: Model II-A - Principal stresses

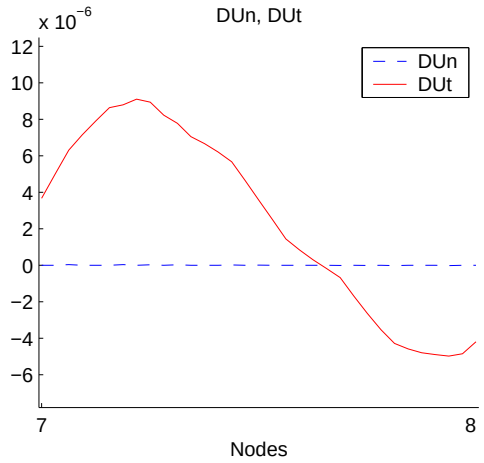

Figure 135: Model II-A - The normal and tangential components of displacement on the contact boundary

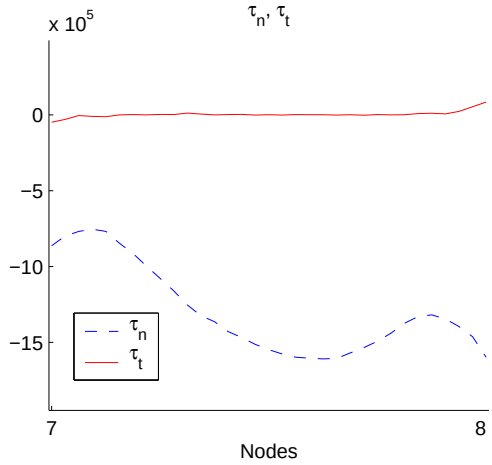

Figure 136: Model II-A - The normal and tangential components of stress vector on the contact boundary

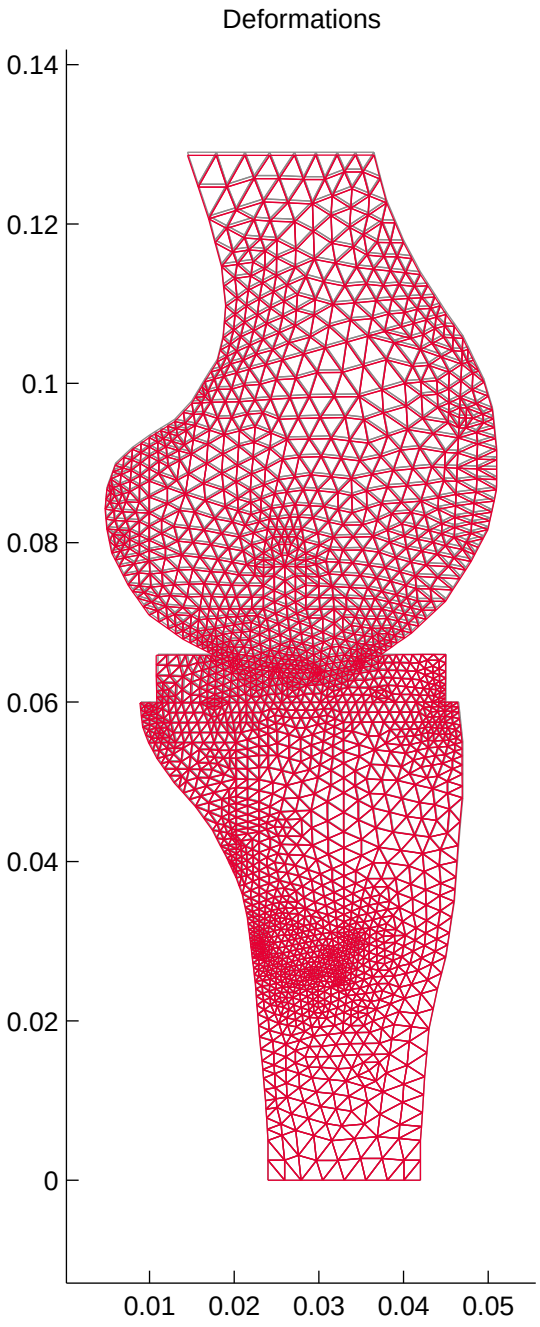

Figure 137: Model II-B - Deformations (enlarge factor=20)

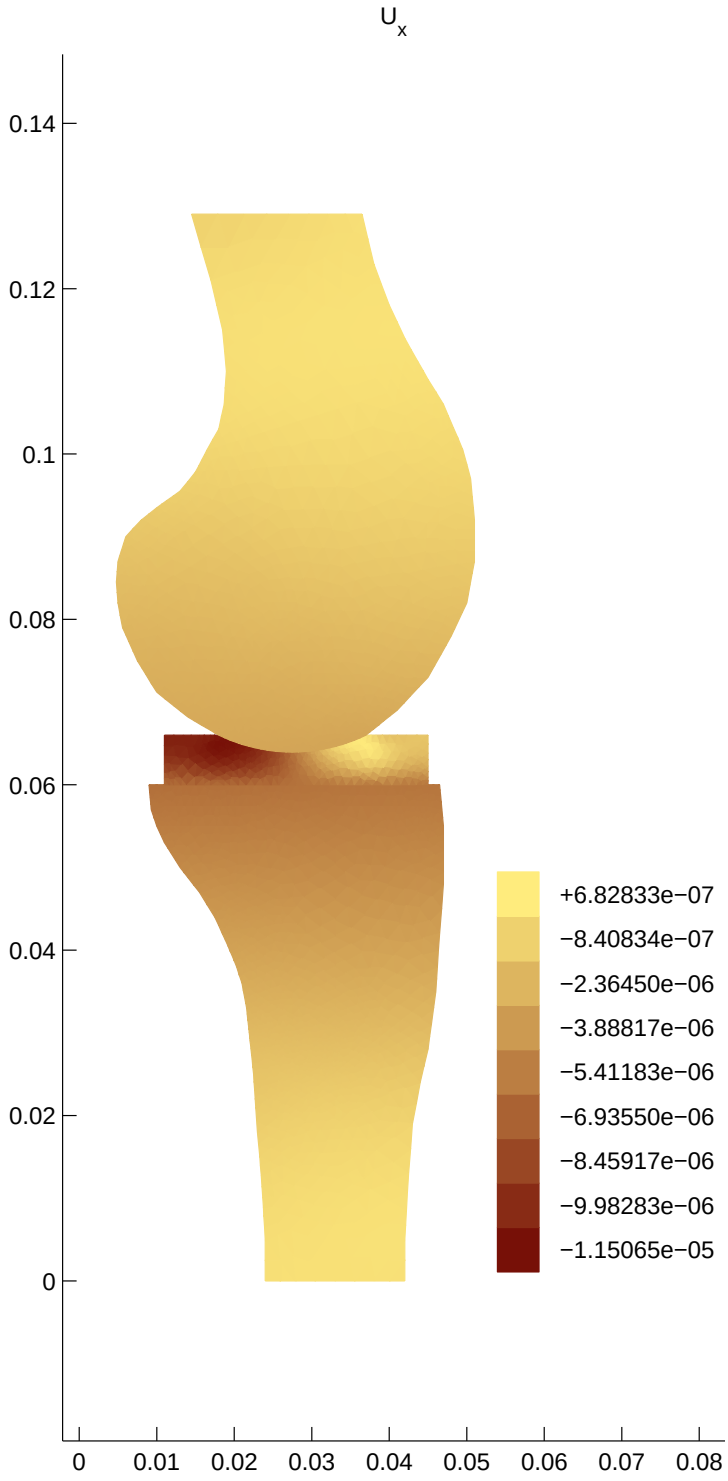

Figure 138: Model II-B - Horizontal component of displacement

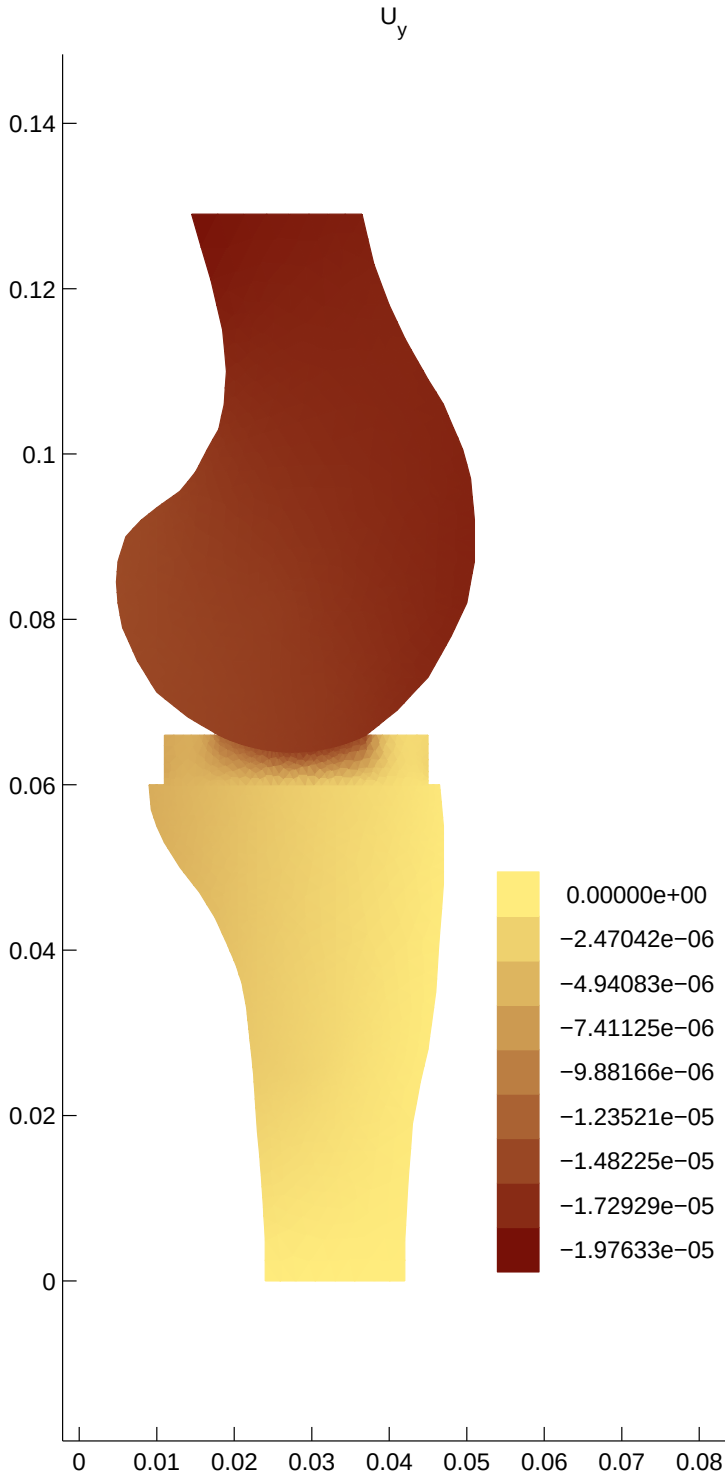

Figure 139: Model II-B - Vertical component of displacement

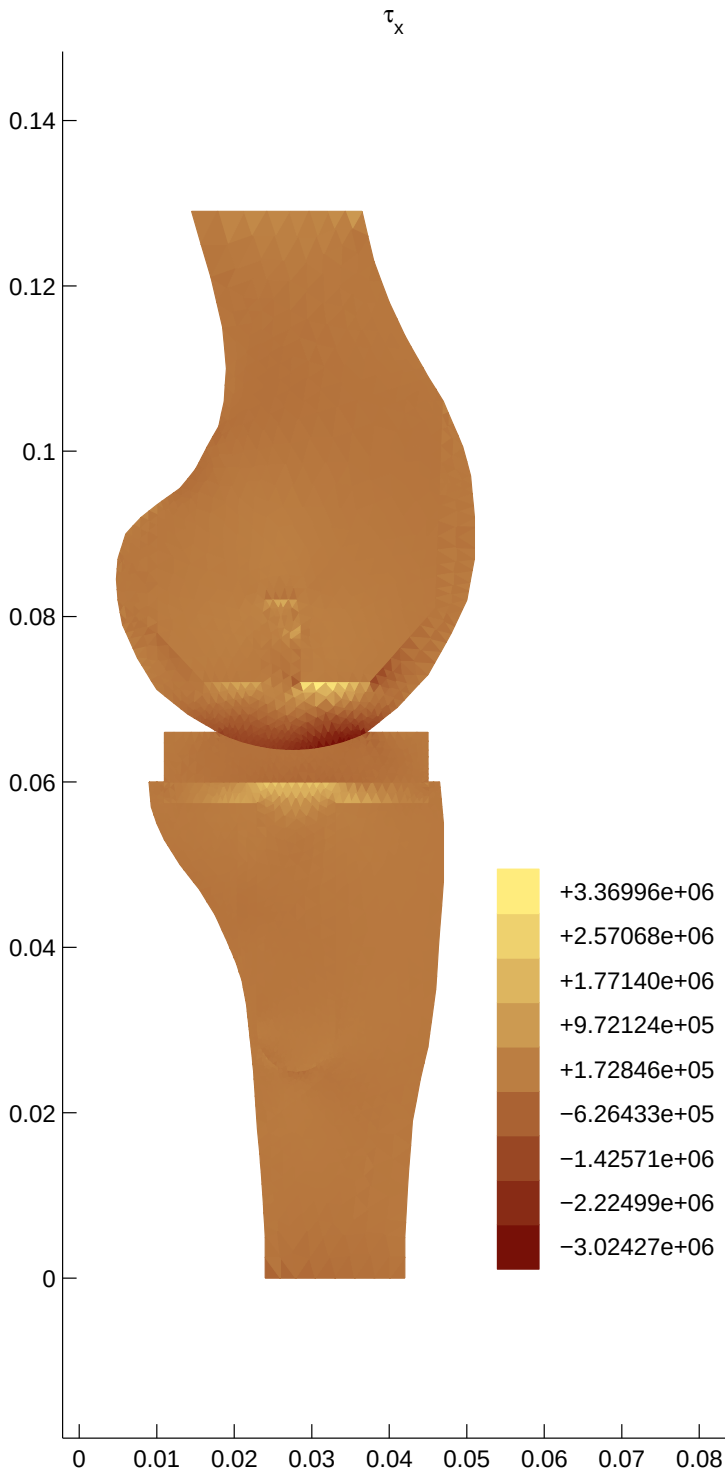

Figure 140: Model II-B - Stresses τ_x

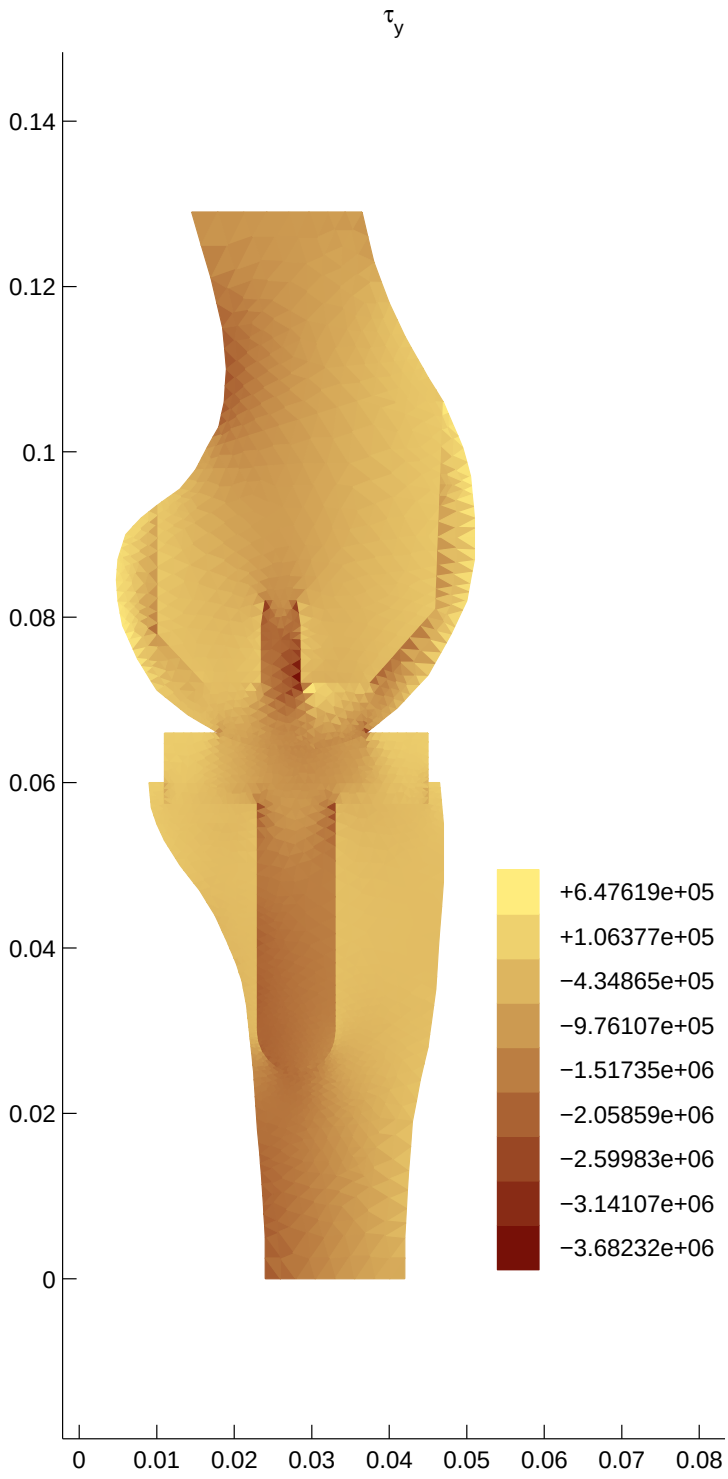

Figure 141: Model II-B - Stresses τ_y

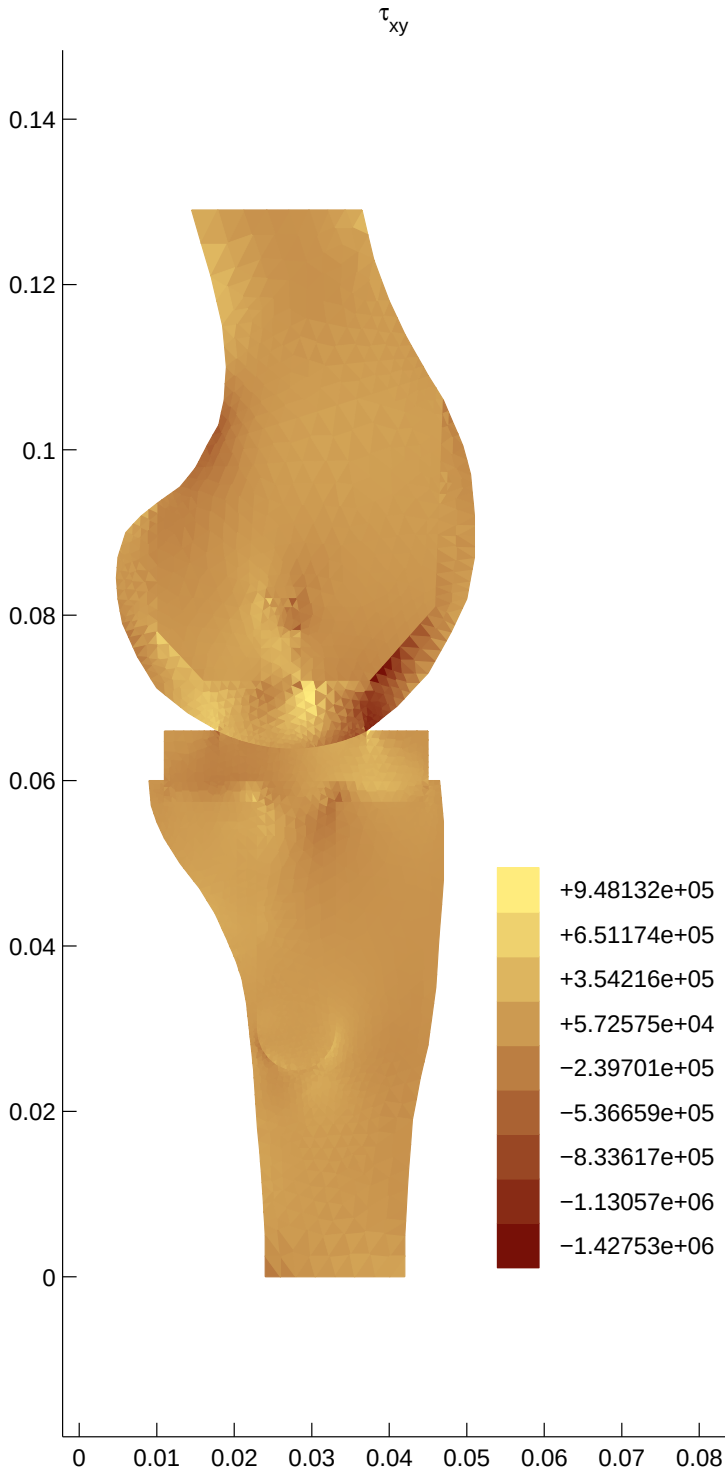

Figure 142: Model II-B - Stresses τ_{xy}

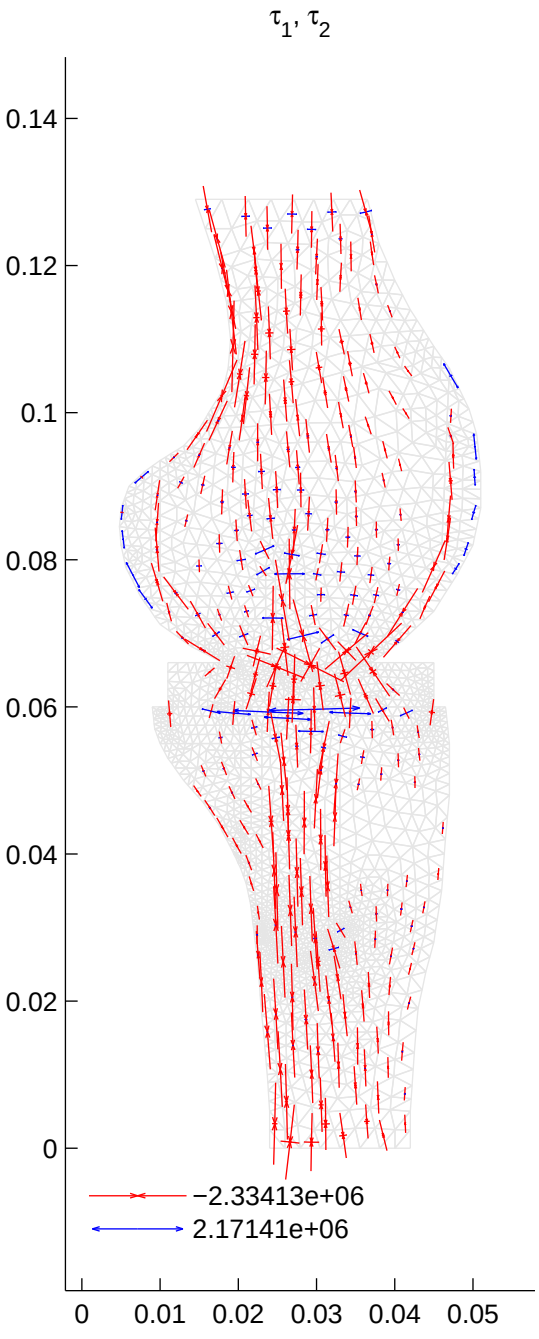

Figure 143: Model II-B - Principal stresses

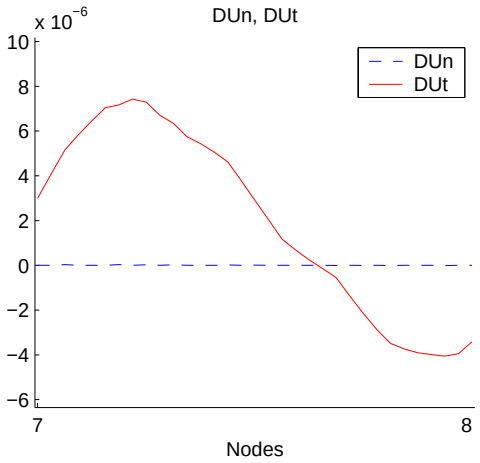

Figure 144: Model II-B - The normal and tangential components of displacement on the contact boundary

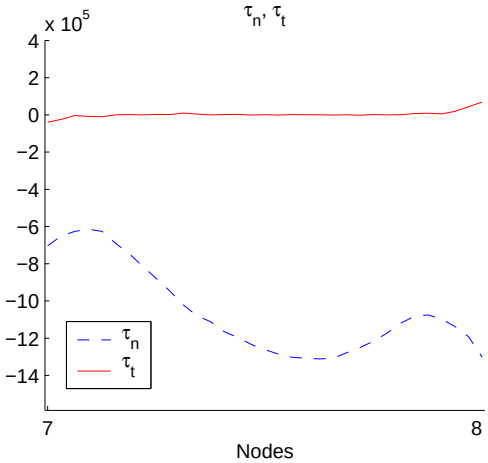

Figure 145: Model II-B - The normal and tangential components of stress vector on the contact boundary

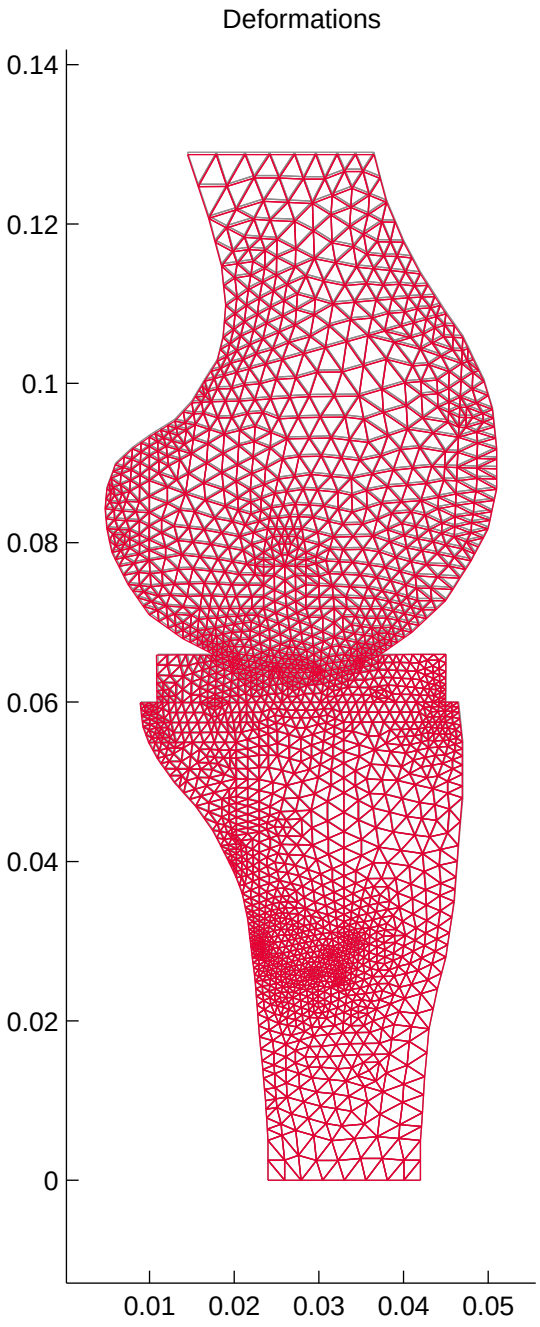

Figure 146: Model II-C - Deformations (enlarge factor=20)

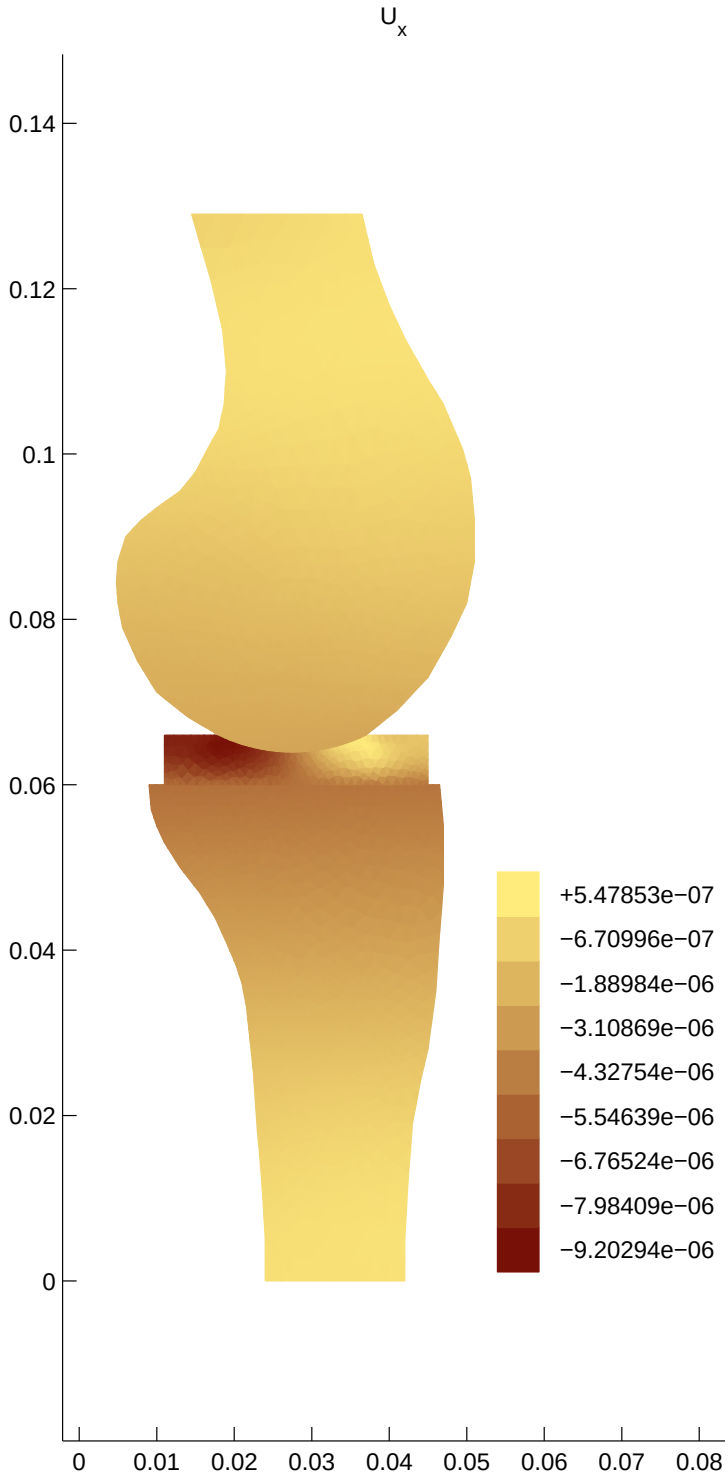

Figure 147: Model II-C - Horizontal component of displacement

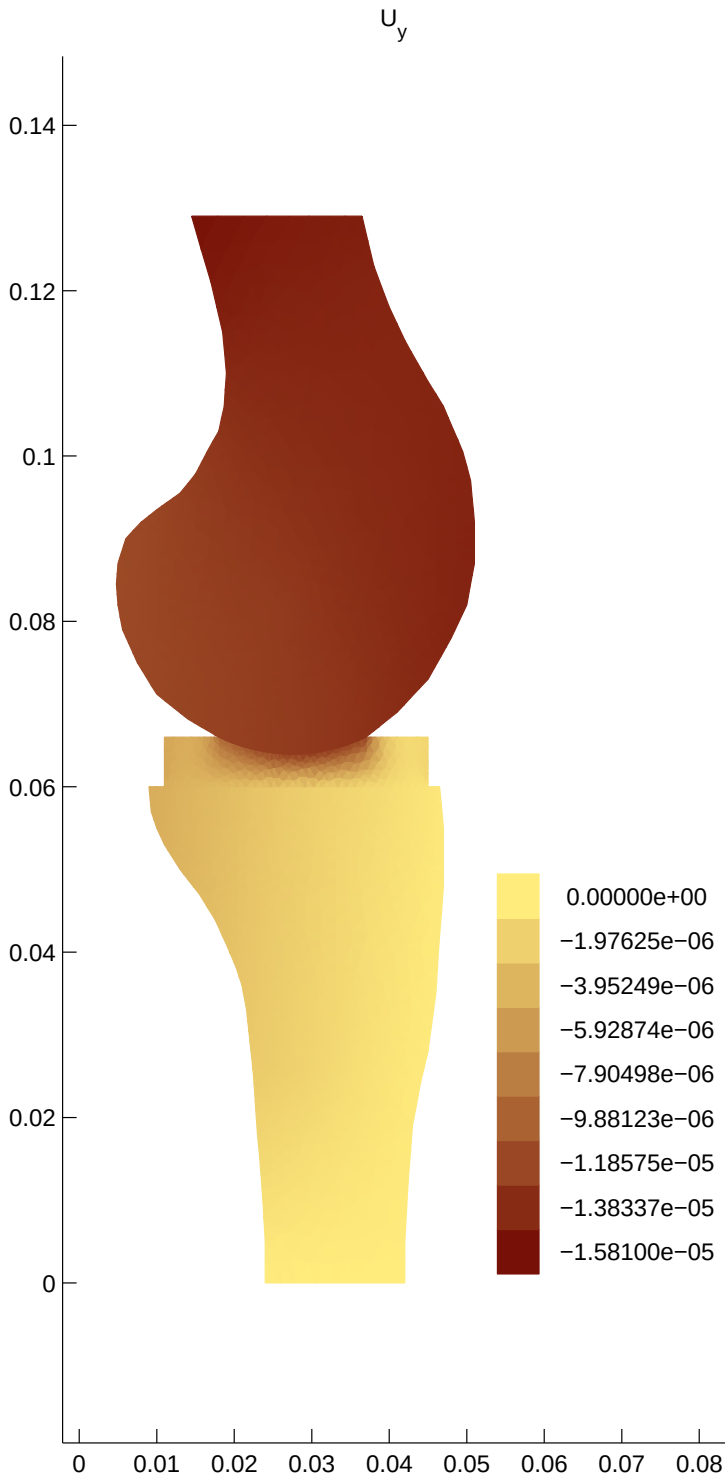

Figure 148: Model II-C - Vertical component of displacement

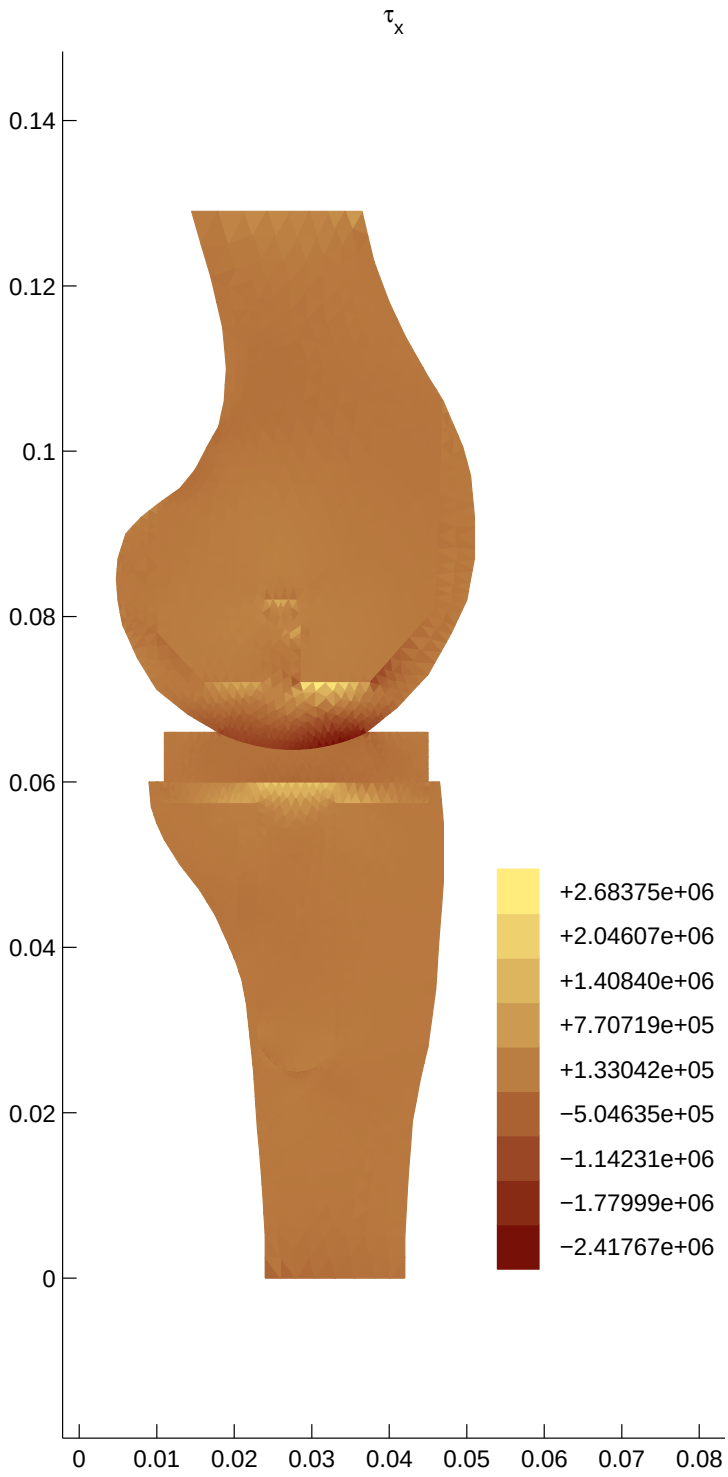

Figure 149: Model II-C - Stresses τ_x

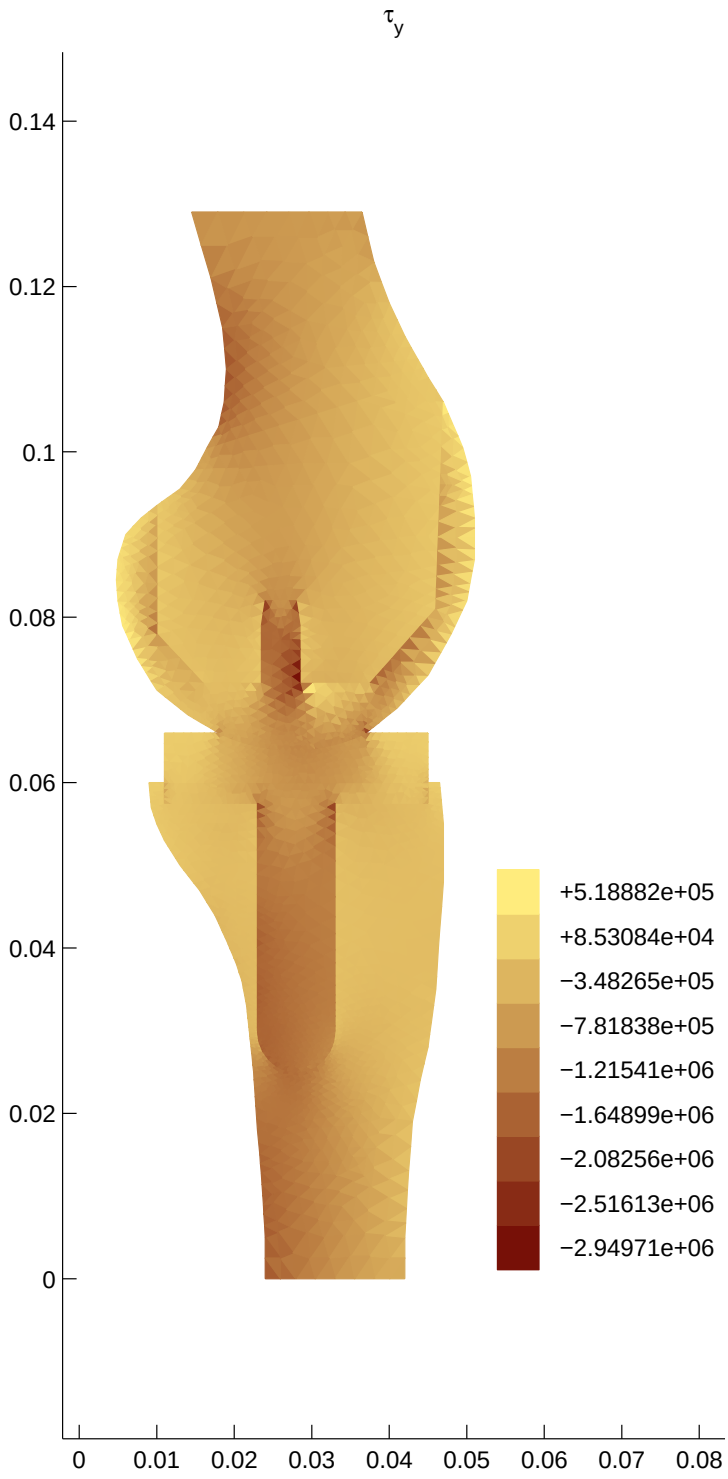

Figure 150: Model II-C - Stresses τ_y

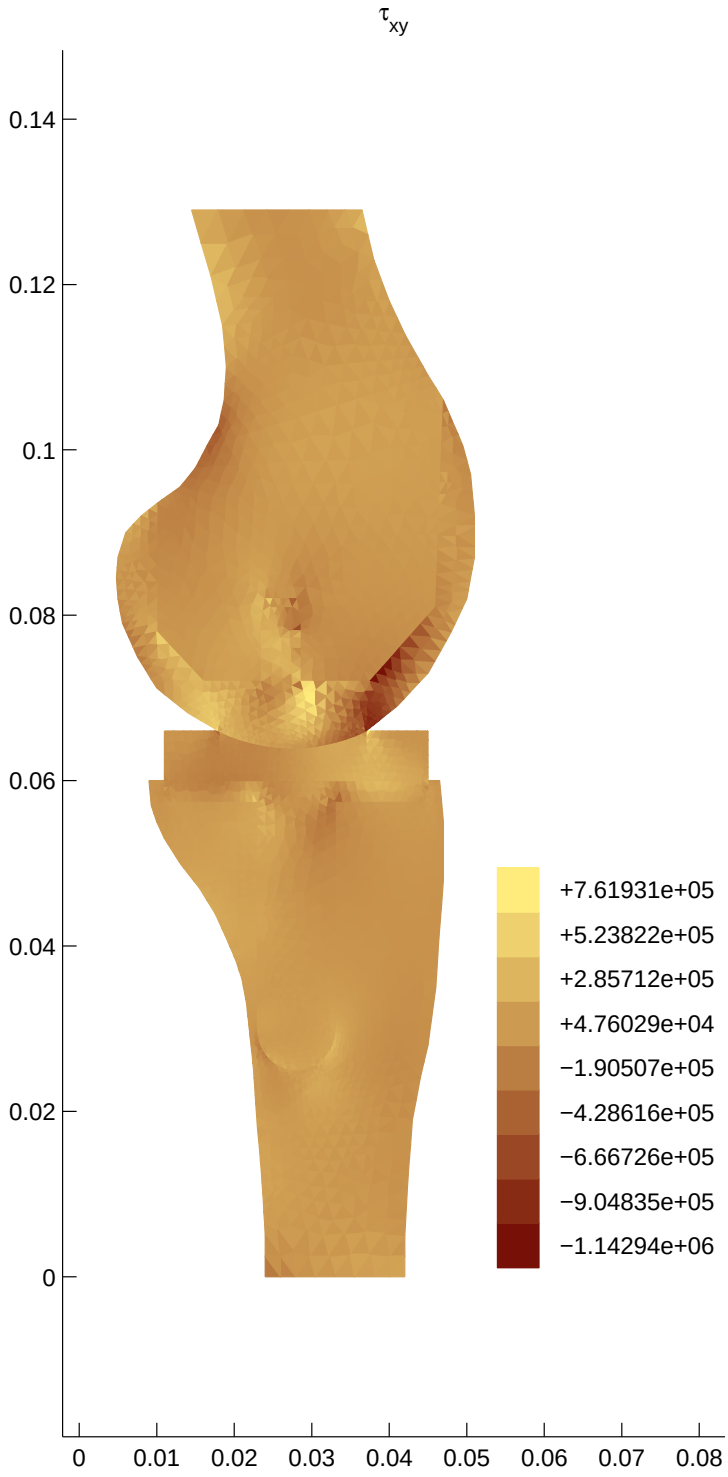

Figure 151: Model II-C - Stresses τ_{xy}

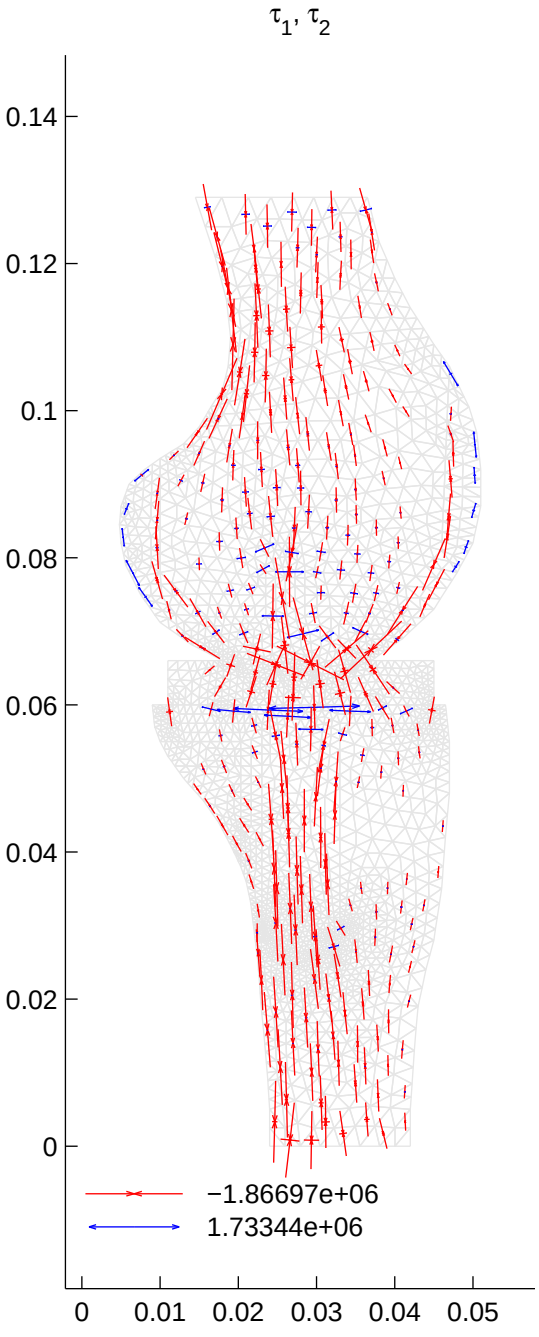

Figure 152: Model II-C - Principal stresses

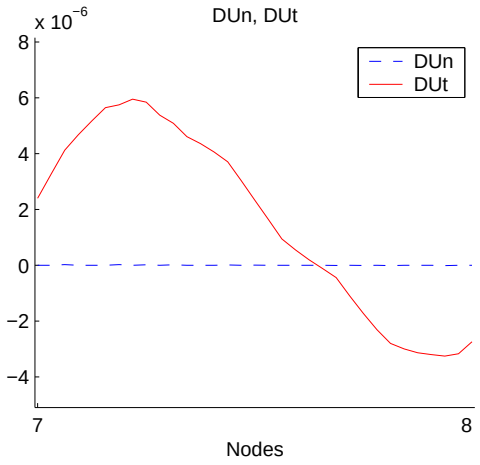

Figure 153: Model II-C - The normal and tangential components of displacement on the contact boundary

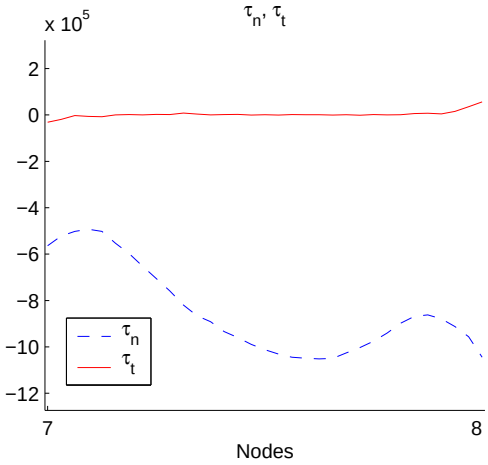

Figure 154: Model II-C - The normal and tangential components of stress vector on the contact boundary